Volume 44 Number 11/12 November 1989

PHILIPS TECHNICAL REVIEW

Compact Disc Interactive

Phosphor screens for projection TV

Electron guns for projection TV

Diagnostic X-ray tube

PHILIPS

Philips Technical Review (ISSN 0031-7926) is published by Philips Research Laboratories, Eindhoven, the Netherlands, and deals with the investigations, processes and products of the laboratories and other establishments that form part of or are associated with the Philips group of companies. In the articles the associated technical problems are treated along with their physical or chemical background. The Review covers a wide range of subjects, each article being intended not only for the specialist in the subject but also for the non-specialist reader with a general technical or scientific training.

The Review appears in English and Dutch editions; both are identical in contents. There are twelve numbers per volume, each of about 32 pages. An index is included with each volume and indexes covering ten volumes are published. This issue includes an index for the last nine volumes.

PHILIPS TECHNICAL REVIEW

VOLUME 44
1988/89

PHILIPS

Philips Technical Review (ISSN 0031-7926) is published by Philips Research Laboratories, Eindhoven, the Netherlands, and deals with the investigations, processes and products of the laboratories and other establishments that form part of or are associated with the Philips group of companies. In the articles the associated technical problems are treated along with their physical or chemical background. The Review covers a wide range of subjects, each article being intended not only for the specialist in the subject but also for the non-specialist reader with a general technical or scientific training.

The Review appears in English and Dutch editions; both are identical in contents. There are twelve numbers per volume, each of about 32 pages. An index is included with each volume and indexes covering ten volumes are published. This volume also includes an index for the last nine volumes.

Subject index, Volume 44, 1988/89

Author index, Volume 44, 1988/89

PHILIPS TECHNICAL REVIEW

Volume 44, No. 11/12, November 1989

Contents

PHILIPS

PHILIPS TECHNICAL REVIEW

Volume 44, No. 11/12, November 1989

A FAREWELL MESSAGE

After very careful consideration we have decided to discontinue the publication of Philips Technical Review. We should explain why we are taking this step.

From its earliest days Philips Technical Review set out to be something special, not just a popular descriptive magazine or another professional scientific journal. The editors' aim has always been to present the material in the clearest possible way, with well-written text and a generous provision of illustrations and graphics. The style is not too academic, and mathematical treatment is kept to a minimum without oversimplifying so far that the treatment becomes vague and superficial.

The great feature of the articles in Philips Technical Review, as compared with those in the professional scientific literature, is that each article in the Review is complete in itself. This means that the subject has to be treated in a wider context, and that the problems arising also have to be described before revealing the solution.

During its fifty years and more the objectives of Philips Technical Review have not changed. But the world has changed, and so too has research. We live in days of increasing specialization. More and more research is done in project groups, often working in cooperation with other companies or in a European context, with team members from a range of disciplines. Describing a project properly — to the high standards of this journal — becomes a more complicated activity, and takes longer, so that the published version may no longer be current. Readers also have to work harder to follow the details of the new developments in a rapidly expanding range of fields.

The changes in research have been matched by changes in the methods of disseminating information. There are more publications with a popular scientific content, and radio and television now have much to offer. We began to wonder whether such a journal was really the best way of presenting news about Philips research.

Considerations such as these led us to the decision to discontinue Philips Technical Review. This was no easy matter, since we have always been rather proud of the Review. And we do realize that we shall disappoint a large number of faithful readers, both inside Philips and outside.

So this is the final issue of Philips Technical Review, an issue strongly oriented toward the future. It discusses the Compact Disc Interactive system, research on high-definition projection television, and a new application of spiral-groove bearings. These subjects show that Philips research and development occupy a leading position in the world, and we firmly believe that the media will continue to keep you informed of our progress.

Thank you for your support and for the interest you have shown in Philips Technical Review.

K. BULTHUIS
Senior Managing Director of Philips Research

Philips Tech. Rev. 44, No. 11/12, 326-333, Nov. 1989

The Compact Disc Interactive system

B. A. G. van Luyt and L. E. Zegers

Two of the terms always associated with the Compact Disc Digital Audio system (CD-DA) are 'digital' and 'laser'. When the system was first introduced in the early eighties it started a real revolution in sound reproduction. In 1987 more than 30 million CD players and 450 million discs were sold. One of the systems derived from CD-DA is CD-I, which has two more special terms associated with it, 'interactive' and 'multi-media', since this system combines images, sound, text and software in an active dialogue with the user.

Introduction

The beam of light emitted by a laser can be focused to an extremely small spot, with a diameter of about a micron. This led to the idea, in the early seventies at Philips Research Laboratories, of using a laser for the recording and playback of information. The extensive research that followed eventually resulted in two new systems:

- LaserVision, for the recording and playback of video information in *analog* form [1].
- Compact Disc Digital Audio (CD-DA), for the recording and playback of audio information in *digital* form [2].

It may help if we briefly consider the similarities and differences between the LaserVision and Compact Disc systems. The most important similarity is that in both systems the signal is recorded on the disc in a long spiral track consisting of a succession of pits about 0.5 μm wide; see *fig. 1a*. The regions between the pits are called 'lands'. The pits are impressed into a plastic substrate by a mould or 'stamper', which is a pressing from a 'mother disc', which in turn is a copy of a master disc. The master disc is the result of 'burning' the information into a 'virgin' disc by a laser. In both systems the pits in the substrate are protected by a transparent layer. Dust and surface damage cannot appear in the focal plane of the 'optical pick-up', which reads the information on the disc in the player.

An essential difference between the two systems is that analog recording is used for LaserVision and digital recording for Compact Disc. Fig. 1*b* shows how the analog signal is recorded on a LaserVision disc. An analog sound signal is superimposed on the frequency-modulated video signal. The resulting signal is limited in both the positive and negative directions. The leading and trailing edges of the blocks produced in this way form the pit/land transitions on the disc. In the CD-Video system derived from LaserVision the sound signal superimposed on the video signal is not an analog signal, but a digital signal.

Fig. 1*c* shows how the digital signal, a sequence of the values '0' and '1', is recorded on a Compact Disc. The length of each pit or land is always a multiple of 0.3 μm. This is different from a LaserVision disc, in which the pit lengths can have an infinite number of values. Every transition from pit to land or vice versa on a Compact Disc forms a 'bit' of value 1. The intermediate bits, which correspond to distances of 0.3 μm on the disc, have the value 0. These 'channel bits' have been produced by coding the original signal bits. These in turn have been produced from a succession

Ir B. A. G. van Luyt is with American Interactive Media Inc., Los Angeles, California, U.S.A., and was formerly with the Philips Consumer Electronics Division in Eindhoven. Dr Ir L. E. Zegers (Deputy Director) is with the Philips Consumer Electronics Division in Eindhoven.

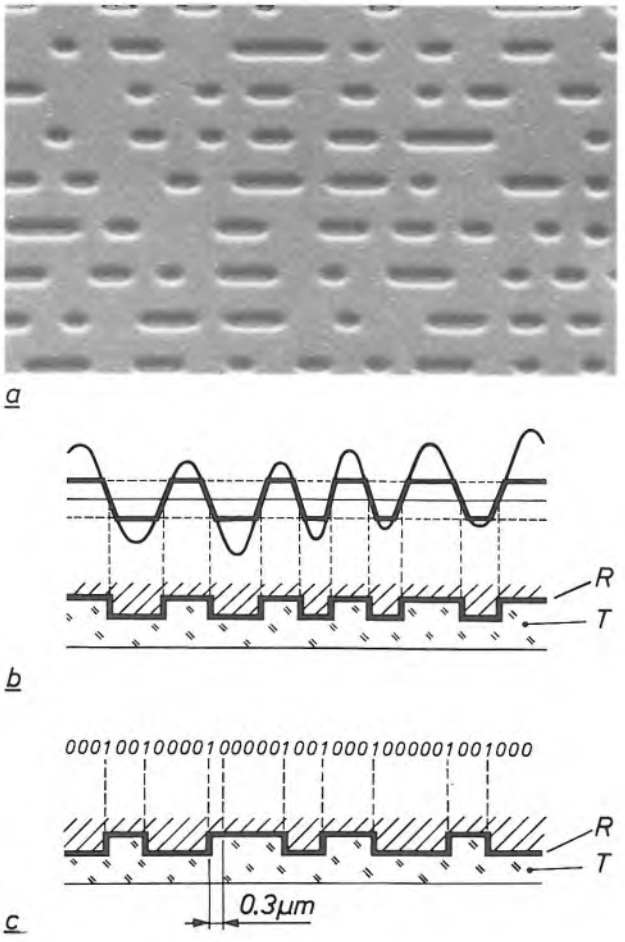

Fig. 1. *a*) The pits and 'lands' (the regions between the pits) in a disc for LaserVision or Compact Disc Digital Audio. The width of the pits is about 0.5 μm. The spiral of pits forms the 'track'. *b*) The conversion of an analog video signal into a sequence of pits and lands in LaserVision. Above: signal; below: cross-section of the disc. The frequency-modulated signal is limited in both positive and negative directions. The leading and trailing edges determine the location of the land/pit and pit/land transitions. *c*) The conversion of a digital audio signal into a sequence of pits and lands in CD-DA. The length of a pit or land is always a multiple of 0.3 μm. Above: bit sequence; below: cross-section of the disc. Every pit/land or land/pit transition corresponds to a '1' in the digital signal. In between the signal always has the value '0' for every 0.3 μm of distance along the track. *R* reflecting layer. *T* transparent material.

of binary numbers that are sampled values of the original analog sound signal: pulse-code modulation or PCM. In the player a decoder circuit converts the channel bits into signal bits, and a digital-to-analog converter converts the signal bits into the analog sound signal.

The great advantage of the digital recording and reproduction of analog information is that it is insensitive to interference and noise. Also, reading errors due to damage or dirt at the surface of the disc can be corrected. The methods for signal processing, and many important quantities such as the dimensions of the disc, have been specified in a CD-DA system standard drawn up by Philips and Sony. Licensing agreements have been concluded with many other companies.

After the successful introduction of the CD-DA system it soon became clear that a Compact Disc was not only exceptionally suitable for recording sound, but could be just as useful for storing digital information for computers. Talks with Sony resulted in a standard for a new kind of memory: CD-ROM (Compact Disc Read-Only Memory). This standard specifies that the digital information shall be organized in blocks, each with an address. Information in one or more blocks can then be traced rapidly and read out from the disc.

The CD-ROM disc is mainly intended for professional and business applications with personal computers. A CD-ROM disc with a diameter of 12 cm can contain about 650 megabytes of digital information. (1 megabyte is $2^{20} \times 8 = 1024 \times 1024 \times 8$ bits.) A disc can contain large numbers of names and addresses or other kinds of text, with a maximum storage capacity equivalent to 150 000 typed A4 pages.

The agreements for the CD-ROM disc have not reached the stage at which the interchangeability of disc and player is guaranteed at all times, as it is for CD-DA. A CD-ROM player is therefore usually a peripheral used with a particular make of computer. A group of companies known as the High Sierra Group have made a number of supplementary agreements relating to the organization of the information on a CD-ROM. These agreements have resulted in uniformity for the tables of contents linking data and addresses. The agreements are set out in ISO standard ISO 9660.

Philips and Sony have gone a step further by drawing up a common standard for a new data-storage system for *consumer application*: the Compact Disc Interactive system, or CD-I. This standard specifies a system and disc that will provide text, images and sound in a real-time dialogue with the user. A system that can offer such an extended range of information is called a 'multi-media environment'. The standard is sufficiently comprehensive to ensure that the disc can be played anywhere at any time.

The agreements embodied in the CD-I standard do not only specify the organization, coding and processing of the data; they also specify the hardware. The CD-I player, which is virtually identical to a CD-DA player, must be connected to an MMC module (MMC

[1] The LaserVision system was originally called 'VLP' (for Video Long-Play); see Philips Tech. Rev. 33, 177-193, 1973.
[2] 'Compact Disc Digital Audio', Philips Tech. Rev. 40, 149-180, 1982.

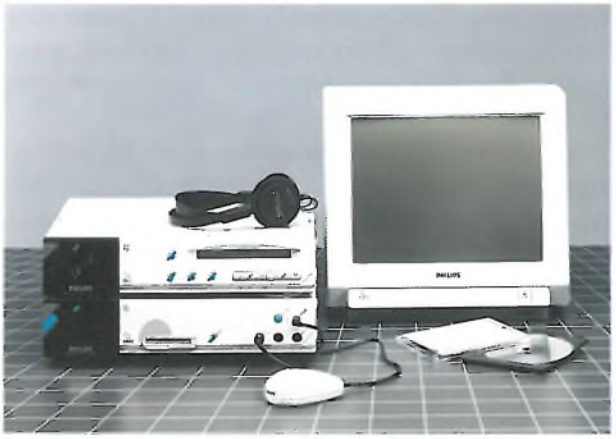

a

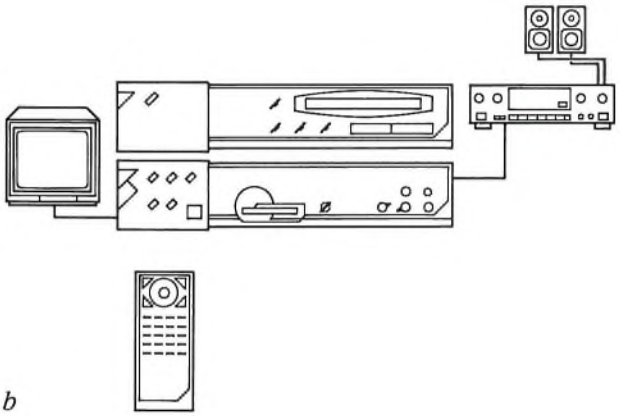

b

Fig. 2. *a*) The CD-I player and the MMC module (Multi-Media Controller). *b*) Block diagram of the hardware. The MMC module decodes the signals for the user's television receiver and audio equipment. The user can communicate interactively with the system, e.g. with a remote control.

stands for Multi-Media Controller), see *fig. 2*. The MMC module contains processors for the video and audio signals and a microprocessor for data management. The module decodes the sound and image information and passes it to outputs connected to the user's television receiver and audio equipment. The data management comes under CD-RTOS (Compact Disc Real-Time Operating System), a special system derived from the OS-9 operating system.

The user gives instructions to his CD-I system by moving a cursor on the screen. He controls the cursor with a controller such as a 'mouse' or a 'joystick'. *Fig. 3* gives an example of the interactive use of an experimental CD-I with the menus shown on the screen. This CD-I was specially made for demonstration purposes.

The CD-I system is the result of extensive experience in optical recording and the interactive use of information systems, gathered from various parts of our company. Here we should mention the experience obtained in compiling an electronic dictionary. This was a joint project shared between our colleagues at CTI (Centre de Technologie Informatique, a Philips company) in Paris and Philips Research Laboratories at Redhill, England [3]. Knowledge already existing within the company about computer operating systems such as OS-9 has been very useful here.

The first working models of CD-I hardware were constructed by the Predevelopment department of the former Home Interactive Systems group (now Interactive Media Systems), in 1985. These models were used in the joint efforts with Sony to establish a system standard. They were also used to specify the requirements for the integrated circuits in VLSI technology (Very-Large-Scale Integration).

Derived versions of these models have also been used as 'authoring systems': 'tools' for suppliers of software for interactive programmes. Authoring systems are necessary for classifying and coding the image, sound and text information. The processed information is then permanently recorded in the stampers for the discs. In the meantime the first CD-Is for demonstration purposes had become available, see for example fig. 3. A first test batch of CD-I hardware was also ready in late 1988.

In the rest of the article we shall first look more closely at the standards for CD-DA, CD-ROM and CD-I. Then we shall discuss CD-I in rather more detail, with a look at the audio and video units and the CD-RTOS control system. Finally, we shall consider future developments.

The standards

Several standards have now been produced:

- The 'Red Book', for CD-DA (1982),
- The 'Yellow Book', for CD-ROM (1985), and
- The 'Green Book', for CD-I (1988).

The Yellow Book and the Green Book are augmented versions of the earlier standards.

In the *Red Book*, blocks of bits resulting from the sampling of an audio signal have blocks of 'parity bits' added to them, according to the rules for the Cross-Interleaved Reed-Solomon Code (CIRC). The blocks of parity bits allow a wide range of errors to be detected and corrected. The data stream is then modulated in Eight-to-Fourteen Modulation (EFM): blocks of eight bits are translated into blocks of fourteen channel bits. The requirement that must be satis-

[3] Valuable contributions to the architecture of CD-I were made by R. Bruno and E. Schylander (Interactive Media Systems Group, formerly known as Home Interactive Systems), J. Taillade (CTI) and S. R. Turner (PRL). Many others contributed to the design of CD-I, including J. Veldhuis (Interactive Media Systems), who created the first CD-I programs.

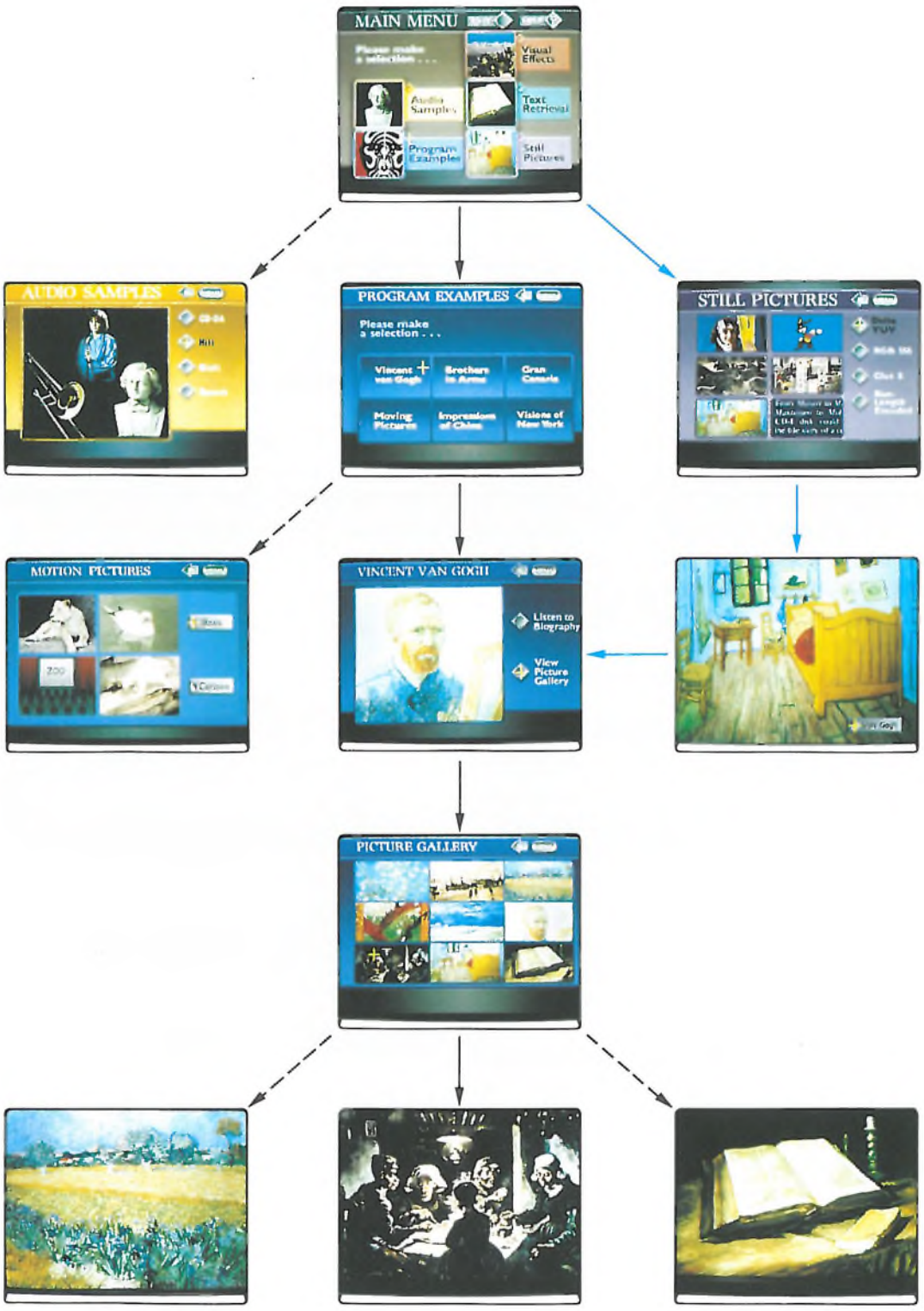

Fig. 3. Example of a CD-I dialogue. The user can find his way about the information on the disc by selecting from menus. The experimental CD-I here contains various examples of CD-I programs and was used for a first demonstration of the system. (The pictures shown here are not representative of the pictures from production CD-Is.) The black arrows correspond to the selections made by the user, as can be seen from the cursor positions. The blue arrows give an example of interactive use: after choosing 'STILL PICTURES' the user has selected a picture by Van Gogh, and has then gone on to obtain information about the painter by selecting 'VAN GOGH'. After the user has selected 'PICTURE GALLERY' and then one of the pictures, it appears on the screen and a reading of a translation of the corresponding letter from the painter's brother Theo is heard from the loudspeaker.

fied here is that sequences of zeros in the resulting stream of channel bits, see fig. 1*c*, must contain a minimum of two zeros and a maximum of ten, always separated by a '1'. Every sequence of zeros plus a '1' corresponds to a pit or land on the disc.

In the *Yellow Book*, the stream of channel bits on the disc is distributed among 'sectors', each containing 2352 bytes of the original information. Each sector starts with the same pattern of synchronization bits to identify the start of a sector. This is followed by a bit pattern representing the sector address and a bit pattern indicating the 'mode'. The sector addresses can be used in a contents list, which can be included at the start of every disc.

The Yellow Book also gives rules for mode designation. In Mode 1 more errors can be corrected than in CD-DA, since each sector contains 288 extra parity bits. This additional provision for error correction is necessary with computer data, and it ensures that no more than one error in a hundred million discs remains uncorrected. Mode 2 does not necessarily have this extra error correction, and is used for storing information in which the consequences of a very occasional error are less serious, such as sound and image information.

The *Green Book* defines the rules for the hardware, system software and the audio and video information in CD-I. These rules ensure that a disc can be used in any CD-I player. The rules for the organization of the information on a disc are mainly based on the Yellow Book. The function of the software is to present interleaved audio, video and text information in real-time dialogue with the user.

The Green Book specifies that in addition to the actual 'header' with the sector address each sector shall contain a 'subheader'. This subheader consists of four bytes, duplicated for extra reliability, and contains information about the type, format and quality level of the data in the sector. One of the functions of the subheader is to permit the real-time presentation of the information on the disc.

A distinction is made in the Green Book between the formats 'Form 1' and 'Form 2'. These offer much the same possibilities for error correction as Modes 1 and 2 in CD-ROM. Since the format designation is included in the subheaders in CD-I, sectors of different format can be interleaved on the disc. Form 1 is used for video information and computer data, Form 2 for audio information and also for video information. A Form-2 sector can contain more information because it does not have the extra parity bits.

Characteristics and applications of CD-I

CD-I has been designed for a multiplicity of applications. These can be subdivided into the following main groups:

- education and training, e.g. language courses, encyclopaedias and 'talking books';
- entertainment, e.g. adventure games and other kinds of interactive games;
- creative leisure, e.g. drawing, painting and composing;
- touring and traffic. This includes consulting maps and tracing out routes. The CARIN vehicle navigation system (CARIN stands for Car Information and Navigation system) makes use of CD-I [4].

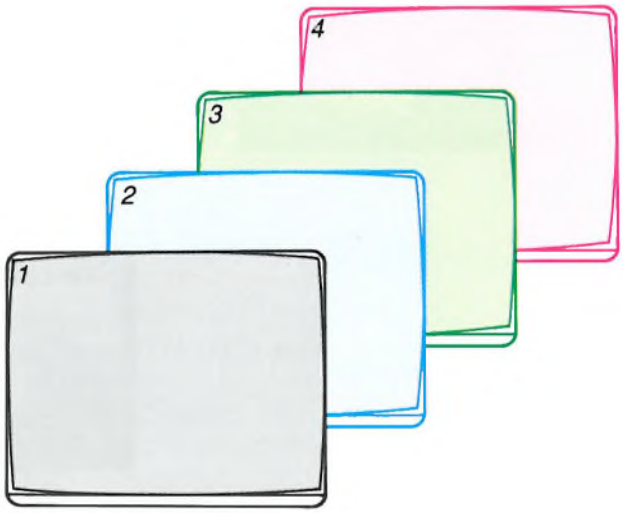

Fig. 4. The four image planes in CD-I corresponding to the four image memories. Image plane *4* can be the background. The image planes can be combined on the screen; when this is done a higher-level image is suppressed, so that it becomes 'transparent'. A lower-level image can then be seen; see also figs 5 and 6.

The organization, digitization and coding of images, sound and text and the provision of paths for interactive use is a time-consuming creative process that requires the use of an 'authoring system'. The result of such a process is a large quantity of digital information on a conventional magnetic recording medium. This is used in making the mother disc in a CD factory.

Companies that are going to supply CD-I programs already have authoring systems. These consist of a CD-I player and MMC module, with extra software

[4] M. L. G. Thoone, CARIN, a car information and navigation system, Philips Tech. Rev. **43**, 317-329, 1987.
[5] R. J. Sluyter, Digitization of speech, Philips Tech. Rev. **41**, 201-223, 1983/84.
[6] M. Nishiguchi, K. Akagiri and T. Suzuki, A new audio bit rate reduction system for the CD-I format, Proc. 81st Audio Eng. Soc. Conv., Los Angeles, Cal., 1986, reprint No. 2375 (C-4), 11 pp.

and hardware. The software is supplied by companies such as the American firm Microware, who also developed the CD-RTOS control system.

In creating and combining the information for a CD-I, a balance has to be struck between the memory space required on the disc and the quality of the images and sound. High-resolution images require more memory space than low-resolution images. This is also true for sound of CD-DA quality compared with sound that only contains the limited frequency range of speech. Various quality levels for sound and image are therefore defined in the Green Book.

Another important factor is the maximum bit rate available at constant playback speed for the track on the disc — the speed is the same for CD-DA and CD-I and is standardized. At this speed a full-screen video picture of broadcast quality, with sound, can be displayed in less than a second.

Audio

A CD-I player can also be used for playing ordinary Compact Discs with their high-quality audio recordings. The high quality of CD-DA is obtained by sampling the analog audio signal at a sampling rate of 44.1 kHz. The number of bits per sample is 32 for each stereo channel, i.e. 16 for each mono channel.

CD-I has different degrees of compression, as compared with CD-DA, for the digitization of the audio signal. The resulting levels of audio quality are:
- hi-fi quality, with double compression, comparable with the first playing of a conventional long-play disc;
- FM quality, with quadruple compression, comparable with the quality of reception for an FM broadcast signal;
- AM quality, with eightfold compression. This is better than the quality of an AM broadcast signal with no interference.

In general, the compression is obtained not by converting the absolute value of each sample into a binary number, but by converting the difference from the previous sample instead. This is differential pulse-code modulation (DPCM)[5]. More accurately, a special form of DPCM is used in CD-I; this is adaptive differential pulse-code modulation, or ADPCM[6]. In ADPCM it is the difference between the actual value of a sample and a predicted value that is converted into a binary number. At the highest quality level the number is an eight-bit number, at the other levels it contains four bits. The predicted value is obtained from previous samples, with the aid of a prediction function that depends on certain slowly varying characteristics of the signal. Sampling rates of 37.8 kHz for the two highest quality levels and 18.9 kHz for the lowest quality level give the stated values for the bit-stream compression.

Fig. 5. Combining two image planes (see fig. 4) as a 'Wipe'. The 'China' image is replaced from top to bottom by the 'Grand Canary' image. The menu offers further visual effects with two images:
- 'Dissolve': one image gradually fades into another;
- 'Curtain': one image replaces another from the left and right, like curtains being drawn;
- 'Blinds': one image replaces another as horizontal stripes of increasing width, like a venetian blind;
- 'Square', one image as a square in another image.

A consequence of the bit-stream compression is that as the quality level falls more audio channels become available. For the highest quality level there are 4 channels (i.e. 4 mono channels or 2 stereo channels), for the second level there are 8 channels and for the lowest there are 16 channels. The information is assigned to the channels a sector at a time.

Video

Three different image resolutions are defined in CD-I:

- normal resolution, comparable with the resolution in an ordinary television receiver,
- double resolution, for the presentation of letters and numbers,
- high resolution, in anticipation of future image-display systems or professional applications.

The CD-I player and the MMC module decode the image information read from the disc so that the signal supplied to the monitor or television receiver represents the correct number of lines: 625 at a frame frequency of 25 Hz, or 525 at a frame frequency of 30 Hz.

Since the maximum bit rate is about 1.36 Mbit/s, it will be necessary to wait a few seconds before a picture appears on the screen, unless special precautions are taken with the digitization of the video signal. This is why advanced compression techniques are used. In CD-I there are four methods of image digitization, each appropriate to a particular kind of image material.

- One-dimensional DYUV coding for 'natural' images, such as a colour photograph. In this method the changes in the luminance signal Y and the chrominance signals U and V of successive pixels are converted into binary numbers line by line.
- Direct RGB coding for high-quality graphics images. In this method a five-bit binary number is assigned to each red, green or blue colour component of a pixel. Each colour component therefore has 2^5 intensity values, so that more than 32 000 different colours can be obtained.
- CLUT coding for graphics images that may need to be changed quickly. A Colour Look-Up Table (CLUT) is included on the disc for this application. This table can contain 2^8, 2^7, 2^4 or 2^3 different colours. The standard provides a choice from a 'palette' of rather more than 16×10^6 shades. In the equipment now available the choice is limited to about 256 000 shades.
- One-dimensional run-length coding with CLUT, mainly suitable for animation. Here use is made of the knowledge that in this kind of application the colour is usually constant over a large part of a line. The binary numbers combine the number of a colour in the table with the number of sequences of pixels in which the colour does not change. Run-length coding can be used to make full-screen moving images.

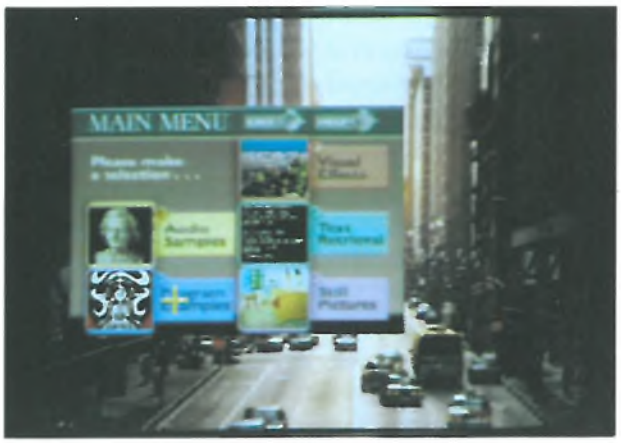

Fig. 6. Another method of combining image planes; see also fig. 4. Image plane *2* is transparent inside the frame, so that image plane *3*, which contains the main menu, becomes visible. Image plane *1* contains the cursor.

The CD-RTOS operating system

The information from each sector is also divided up into channels for other kinds of information besides sound. The CD-RTOS operating system ensures that the data stream read from the disc is divided appropriately and sent to different outputs as required. With the information distributed over the channels in this way speech signals in various languages can be included on the disc and therefore in the data stream. When the user chooses a language in his dialogue with the system, CD-RTOS ensures that the appropriate channel is connected to the audio output.

For combining images, the system has four 'image planes'; see *fig. 4*. Images to be combined are stored temporarily by CD-RTOS in image memories. Various dynamic effects with images can be produced in this way; see *fig. 5*. Images can also be built up from parts of other images or images can be superimposed. If desired, parts of an image plane can be made 'transparent', so that a lower image plane is made visible; see *fig. 6*. The lowest image plane can be used as the background.

As stated, each sector can contain audio, video or text information, or software. Information recorded in the subheader of each sector indicates how CD-RTOS should interpret the information in that sector. The address information in the header can be used by the operating system or the user for searching. Interactive searching is a feature of CD-I; see fig. 3.

It will be clear that information in the data stream read from the disc can be interleaved with related information. After the data stream has been sorted out, CD-RTOS sends it to the correct output channel in real time. Facial movements in the image, for example, must correspond exactly with the speech; in other words the information from the video output must be synchronized with that from the audio output.

Current status and further developments

It will have become clear from what we have said that the development of CD-I is a team effort, with contributions from colleagues from various disciplines. The first phase of the development, in which the notable feature was the close cooperation with the Philips research laboratories, included the following activities:

- drawing up a standard,
- producing prototypes,
- specifying integrated circuits in VLSI technology,
- preparation for production.

The activities listed above mainly concern the hardware and the associated software. Experience has shown that it is no use introducing hardware if the data carriers are not obtainable in sufficient variety. Considerable effort has therefore been put into developing authoring systems and supplying them to companies that make programs for the discs. We want to offer users a wide choice of interesting interactive applications in the near future.

A technical challenge that must soon be faced is that of finding more effective compression techniques, to give further improvement in the quality of moving images. At the same time second-generation integrated circuits will have to be developed. Simpler hardware will then be within reach. The ultimate results will be reductions in price and a corresponding increase in the scale of production, with increasing diversification in hardware and discs.

Summary. The standard for the CD-I system (Compact Disc Interactive) for consumer applications is an extension of the standard for CD-ROM (Read-Only Memory) for professional applications for computers, which in turn is an extension of the standard for CD-DA (Digital Audio). The CD disc contains images, sound, text, and the associated software in digital form. The information is organized in sectors on the disc, each with its own address and a list of contents. There are two levels of error correction, four quality levels for sound and three quality levels for images. This means that quality can be traded against storage capacity and bit rate when the disc is created. The supplier of interactive programs does this by means of an authoring system. The output from the authoring system is the digital information used in manufacturing the 'mother disc'.

1939 THEN AND NOW 1989

Television receivers

Philips have been designing television receivers for more than fifty years. The console model in the black-and-white photograph [*] was 80 cm high, with the cathode-ray tube and the loudspeaker mounted one above the other. The set was tuned to receive the BBC transmissions from London. These provided an interlaced 405-line picture, with 25 pictures a second. In those days the picture tube had rotational symmetry, and the slightly rounded screen face had a diameter of 22 cm. The picture height was 15 cm and the width was 17.5 cm.

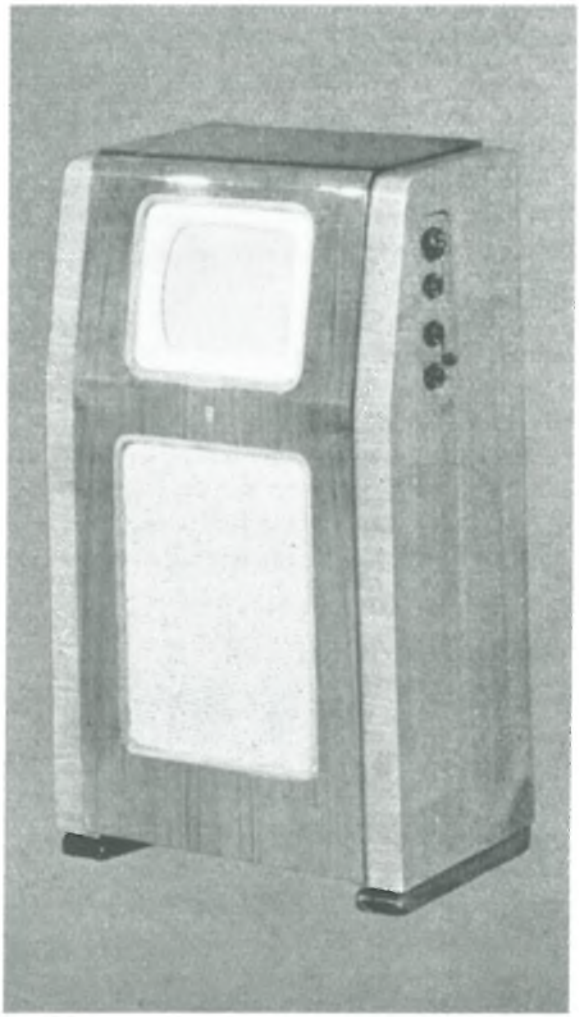

Much has changed since that time. The photograph below shows the 28DC 2070 colour television receiver that became available this autumn. The rectangular 625-line picture measures 53 cm by 40 cm; the screen is flat and square and there is not a control to be seen — the set is operated entirely by remote control. The loudspeakers can be positioned separately. Connections are available for video recorder and computer.

The inside has changed too, not just the outside. Most of the discrete components have been replaced by ICs, and the set also contains a number of modules that add new features. One of these is hi-fi stereo sound, made possible by digital signal processing. The receiver also offers PIP (Picture in Picture), which shows a 18 cm by 12 cm picture of another programme simultaneously in a corner of the screen. There is a teletext module, of course, with an 8-page memory in this model.

Work on the television of the future continues, and further changes are just around the corner. One such will be the aspect ratio of the screen — from about 4:3 to 16:9.

The greatest step forward, however, will be the improved viewing with D2-MAC; the resolution will be better, and there will be fewer artefacts, since there will be less crosstalk between the chrominance and luminance signals in the transmitted signal. And the HD-MAC standard will be introduced later, with a 1250-line picture.

[*] From Philips Technical Review, December 1939.

Phosphor screens in cathode-ray tubes for projection television

R. Raue, A. T. Vink and T. Welker

Cathode-ray tubes with phosphor screens have been used for picture display since the early days of television. The conventional direct-view tube for colour television contains a screen with three phosphors that give red, green and blue light when they are excited by electrons. In projection television, colour display is obtained by superimposing the magnified images from three separate tubes on a large viewing screen. The requirements for the phosphor screens are much harder to meet than in a direct-view tube, because of the high excitation densities. The renewed interest in projection television will certainly be strengthened by recent improvements in phosphor screens to give much better picture quality.

Introduction

The phosphor screens in the cathode-ray tubes in television receivers convert the energy of fast electrons into light. In conventional direct-view television the viewer looks directly at the picture produced on the tube faceplate, but in projection television the image is projected on to a large viewing screen — an attractive way of displaying high-quality pictures with a diagonal of 100 cm or more. For projection television in colour, three separate cathode-ray tubes produce images in the primary colours red, green and blue. These images are projected in exact register with the aid of electronic control.

Recent improvements in picture quality have led to an increased interest in projection television, and this will receive a further stimulus from the introduction of high-definition television (HDTV) with large picture formats. In a previous article in this journal [1] it was shown how the brightness and colour rendering (chromaticity) can be improved by applying interference filters to curved faceplates. In this article we shall discuss the phosphor screens to be used.

A phosphor screen in a projection-television tube is used in much the same way as the screen in a direct-view tube. A phosphor layer deposited on the faceplate is covered by a thin aluminium film that acts as an electrode and also reflects light forwards. Electrons arriving from the back of the screen pass through the aluminium film and into the phosphor layer. The light generated by the electron excitation leaves the phosphor screen from the front after reflection and scattering.

Pictures with sufficient brightness and resolution for projection television are obtained by excitation with an intense and very small electron spot. The diameter of this spot is about a tenth of the diameter of the spot in present direct-view tubes, and the maximum excitation density ($\approx 2\,W/cm^2$) is about a hundred times higher. This sets very difficult requirements for the phosphor screens. If the screen is to give optimum performance, it is necessary to consider the luminescence properties of phosphors under the conditions encountered in projection television, the suitability of a phosphor for screen preparation, and the optical properties of the screen.

Properties of importance in projection television are the energy-conversion efficiency (particularly at high excitation densities), the 'chromaticity coordinates', the decay time and the thermal quenching,

Dr R. Raue and Dr T. Welker are with Philips GmbH Forschungslaboratorium Aachen, Aachen, West Germany, and Dr Ir A. T. Vink is with Philips Research Laboratories, Eindhoven.

[1] L. Vriens, J. A. Clarke and J. H. M. Spruit, Interference filters in projection television tubes, Philips Tech. Rev. 44, 201-210, 1989.

and the variation in properties under prolonged intense electron bombardment. The requirements for chromaticities and decay time are the same as in direct-view tubes. This means that the chromaticity coordinates of the phosphors (including the effect of interference filters) should meet the European Broadcasting Union specifications for red, green and blue to ensure faithful colour reproduction, and that the decay time should be short enough to avoid 'smearing' in moving images. The efficiency should be as high as possible. Some of the efficient phosphors used in direct-view television are not suitable for projection television, however, because the light output saturates strongly at high excitation densities. It is therefore also necessary to consider phosphors that are less efficient at low excitation densities but better at high densities because they are more linear. The requirements relating to thermal quenching and deterioration in efficiency are also more difficult than in direct-view tubes.

The suitability of a phosphor for use in a screen depends on the type of layer required. A typical screen has an average thickness between 10 and 30 μm and consists of a powder with a mean grain size between a few μm and about 10 μm. It is also necessary to optimize the size distribution about the mean grain size. The morphology of the grains should not be so complex that it is impossible to obtain the high packing density necessary for stability at high excitation densities and for good optical properties of the screen. Finally, the phosphor must not be affected by the screen processing.

The optical properties of a screen depend closely on the thickness of the phosphor layer. At a given packing density of the phosphor, the layer must be thick enough to ensure sufficient absorption of the electron energy. A limit to the thickness is set, however, by multiple light scattering in the layer. In a thick layer much of the light is lost owing to scattering and subsequent absorption in the phosphor screen, and the sharpness of the image (resolution) is reduced by lateral scattering. However, some scattering is necessary to give a gain in brightness in the forward direction. This scattering depends on the size and morphology of the grains and on the index of refraction of the phosphor. In current phosphors the grain size is the dominant parameter. Prolonged electron bombardment often leads to additional light absorption due to 'browning' of the screen; its effect is increased by multiple light scattering. The browning may be affected by the screen processing.

In this article we shall compare phosphors for projection television with phosphors used for direct-view screens, and we shall present a model for the analysis and prediction of optical screen properties. We shall also review the screen processing and discuss the degradation of phosphor screens in projection-television tubes. Finally, we shall look briefly at the future prospects.

Phosphors for projection television

The physical processes involved in the electron excitation of a phosphor are presented schematically in *fig. 1*. A phosphor basically consists of a 'host lattice' and an 'activator', a general term for elements incorporated to activate the luminescence. Fast electrons penetrate the phosphor and are slowed down by the increasing interaction with the host lattice. The penetration depth increases with the acceleration voltage and decreases with the density of the phosphor; typical values of the penetration depth for 30-kV electrons, as used in projection television, range from 3 to 5 μm. The electrons excite inner shells of the host-lattice atoms and the resulting energetic electrons generate secondary electrons. Eventually electron-hole pairs are formed in the host lattice and these can transfer their energy to the activator ions, which are then excited to emit light. Unfortunately there are also a number of loss processes such as energy transfer to 'killer centres', surface recombination at the 'dead layer', and non-radiative deactivation in the activator ions.

Ideally the three phosphors that emit the red, green or blue light should have high efficiencies up to high

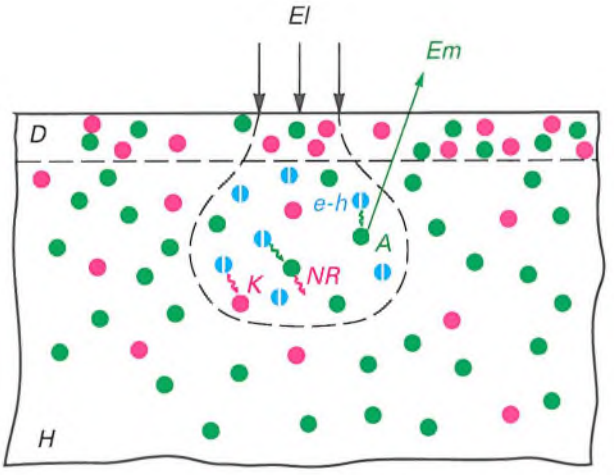

Fig. 1. Diagrammatic representation of the luminescence produced in a phosphor grain by electron excitation. Accelerated electrons *El* are incident on a host lattice *H* containing activator ions *A*. The incident electrons are absorbed in the host lattice; the penetration range increases with the acceleration voltage. The absorption of electron energy results in the generation of electron-hole pairs *e-h*. These can transfer their energy to the activator ions, which can be excited to give light emission *Em*. No luminescence is generated in a thin region near the surface, the 'dead layer' *D*. Unwanted processes also arise, such as energy transfer to killer centres *K* and non-radiative deactivation *NR* in the activator ions.

excitation densities, as well as the correct chromaticities and decay times. Thermal quenching and deterioration with time should also be negligible. In practice the choice is a compromise, mainly determined by the balance between the efficiency and linearity of the phosphor, provided the other properties are acceptable. It can therefore happen that the 'best choice' may change with time because of changing tube and system requirements in the future, e.g. for the scanning conditions. It is therefore important to present the luminescence properties in such a way that the performance of the tubes for blue, green and red in various combinations can be predicted. We shall now go on to discuss the basic essentials of the spectral properties and efficiency of the luminescence, sublinearity at high excitation densities, and an experimental comparison of some of the phosphors that could be used in projection television.

Spectral properties and efficiency

The combination of host lattice and activator determines the luminescence properties of a phosphor. Emission spectra for several phosphors are shown in *fig. 2*. The blue emission of ZnS:Ag (also used in direct-view tubes) is broad; this is ascribed to the strong interaction between the silver activator and the host lattice. In the same way the green-emitting direct-view phosphor $Zn_{0.95}Cd_{0.05}S$:Cu, indicated by (Zn,Cd)S:Cu, gives a broad-band emission. For projection television, however, a green-emitting Tb^{3+}-activated oxidic phosphor is preferred. This phosphor emits in spectral lines, as does the phosphor Y_2O_3:Eu, used for red in projection television.

The line emission of phosphors activated with Tb^{3+} or Eu^{3+} indicates that the interactions between these activators and the host lattice are very weak [2]. These interactions are very weak, because of the special nature of these rare-earth ions: the luminescence transitions take place inside their inner 4f shells, which are well shielded from the environment by outer electron shells. The mutual interactions between these ions are also very weak, which means that they can be used at concentrations of up to 1-10% without serious loss in efficiency due to concentration quenching. Their behaviour is different from ZnS:Ag and (Zn,Cd)S:Cu, where concentration quenching limits the useful activator concentration to about 0.05%.

In our discussion of the energy-conversion efficiency we shall first consider the various stages in the excitation process; see *fig. 3*. Electron-hole pairs are generated by the incident fast electrons [3], and it has been found that the generation of one thermalized electron-hole pair requires an average energy βE_g,

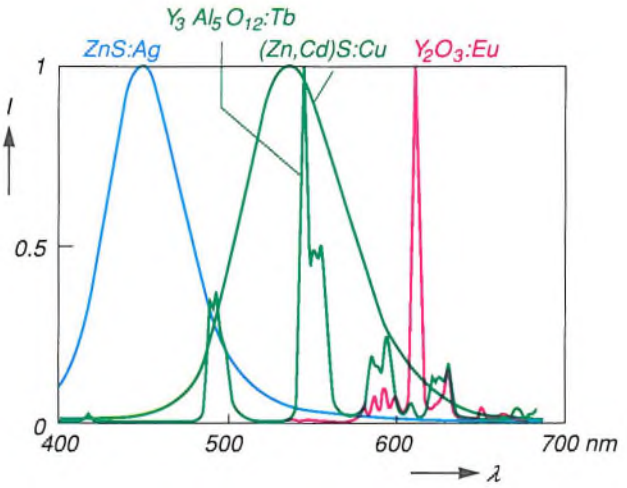

Fig. 2. Emission spectra produced in phosphors by cathode-ray excitation. The normalized photon intensity I is shown as function of the wavelength λ. The spectra of the blue-emitting ZnS:Ag and the green-emitting (Zn,Cd)S:Cu are broad; the spectra of the green-emitting $Y_3Al_5O_{12}$:Tb and the red-emitting Y_2O_3:Eu consist of sharp lines.

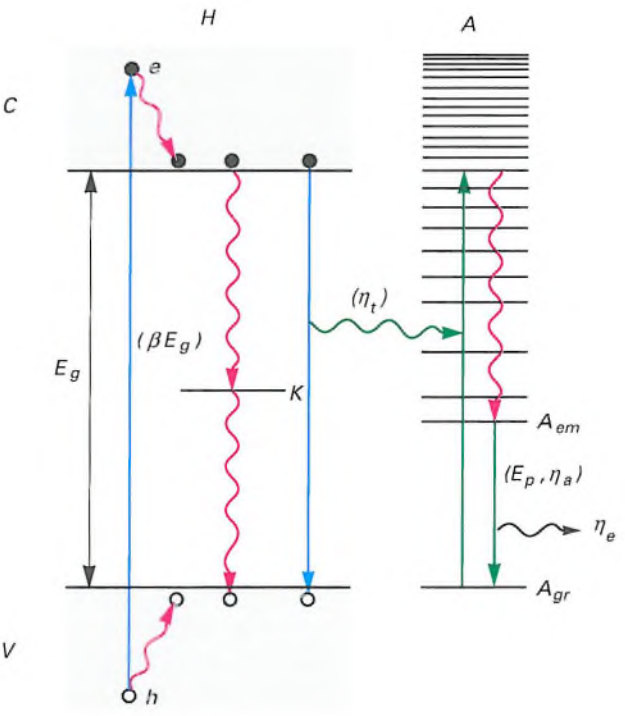

Fig. 3. Different stages in the electron excitation of a host lattice H with activator ions A. The generation of a thermalized electron-hole pair formed by a hole h in the valence band V and an electron e in the conduction band C requires a mean energy βE_g, where E_g is the band gap of the host lattice. Electrons in the conduction band can recombine with holes in the valence band via killer centres K or via energy transfer (at an efficiency η_t) to the activator. The activator returns from its excited state to the emitting state A_{em} via non-radiative transitions. The return to the ground state A_{gr} then causes the emission of light at a photon energy E_p, a quantum efficiency η_a (the ratio of the number of photons generated to the number of activator ions excited) and a photon-escape efficiency η_e.

[2] See for example G. Blasse and A. Bril, Characteristic luminescence, Philips Tech. Rev. 31, 303-332, 1970.

[3] D. J. Robbins, On predicting the maximum efficiency of phosphor systems excited by ionizing radiation, J. Electrochem. Soc. 127, 2694-2702, 1980.

where E_g is the band gap and β ranges from about 2.7 to 5, depending on the host lattice. The next step is the transfer of the electron-hole energy to the activator, with an efficiency of η_t. The excited activator then relaxes to its luminescing state and returns to its ground state. This leads to the emission of a photon of energy E_p, with a quantum efficiency η_a and an efficiency η_e for escape from the phosphor powder or phosphor screen.

If we consider the different stages we can estimate the energy-conversion efficiency η_{CR} for cathode-ray excitation:

$$\eta_{CR} = \frac{E_p}{\beta E_g} \eta_t \eta_a \eta_e. \qquad (1)$$

The maximum efficiency is obtained when η_t, η_a and η_e are all unity. It is advantageous if the values of β and E_g are as small as possible, but the value of E_p is fixed by the emission colour required. For ZnS:Ag we have $E_g = 3.8$ eV, $E_p = 2.7$ eV and $\beta = 2.7$, so that the theoretical maximum of η_{CR} is 26%. The highest efficiencies obtained with this phosphor are close to this value. Oxidic host lattices such as $Y_3Al_5O_{12}$ have larger values for E_g and β, and therefore have lower efficiencies. The highest value obtained with green-emitting $Y_3Al_5O_{12}$:Tb is about 10%, whereas with (Zn,Cd)S:Cu efficiencies of up to 18% can be obtained. These efficiency values are associated with the conversion of the absorbed electrons; the conversion efficiency of the incident electrons is only 80 to 90% of these values because of electron back-scattering.

Since the excitation densities are high in projection television, the screen temperature can rise significantly, and may even reach 100 °C. This implies that the decrease in efficiency with increasing temperature (thermal quenching) should be small. This quenching is mostly due to non-radiative losses from the emitting state and depends on the coupling to the lattice vibrations [2]. Although models are available that explain these processes, it is difficult to make accurate predictions. However, a knowledge of the measured temperature dependence of the efficiencies enables us to select phosphors with negligible losses at 100 °C. A more serious problem with high excitation densities is the sublinearity of the luminescence output.

Sublinearity

To demonstrate the sublinearity we show the efficiency of several phosphors in *fig. 4* as a function of the excitation density, i.e. the energy density of the excitation pulse, at typical values for projection tubes and direct-view tubes. The efficiencies of phosphors such as ZnS:Ag and (Zn,Cd)S:Cu fall off considerably at higher excitation densities. On the other hand

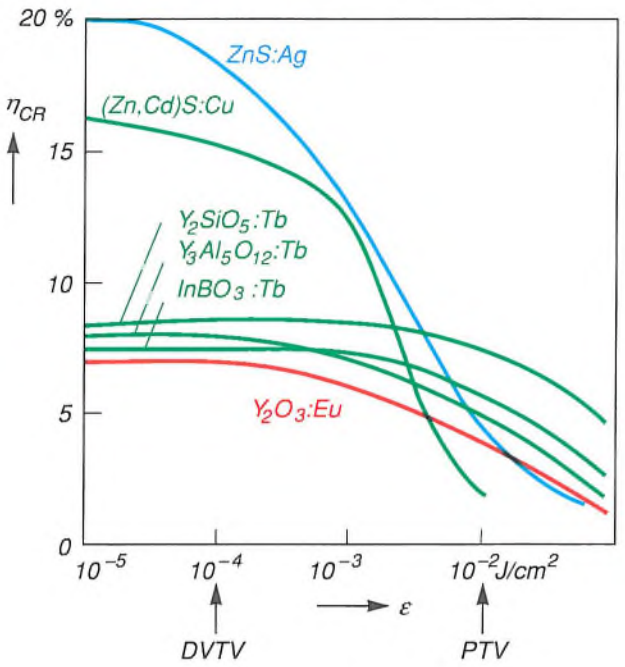

Fig. 4. Energy-conversion efficiency η_{CR} of various phosphors as a function of the excitation loading, i.e. the excitation density per pulse (ε), in a projection-television tube at a fixed electron spot diameter. The efficiency of the phosphors ZnS:Ag and (Zn,Cd)S:Cu, which is high at low excitation loadings, decreases strongly at higher loadings. The arrows indicate typical values of ε in direct-view television tubes (*DVTV*) and in recent projection television tubes (*PTV*).

the Tb^{3+} and Eu^{3+} phosphors have lower efficiencies at lower densities, but at higher densities they have the advantage of superior linearity.

As long ago as 1949 [4] a model was proposed that would explain the sublinearity of phosphors such as ZnS:Ag. We can describe the basic features of this model with the aid of fig. 3 and eq. (1), and note that the electron beam scans the phosphor screen in lines, thus giving excitation of each picture element in short pulses. The pulses have a typical duration of 200 ns, and are repeated at 40-ms intervals. Most phosphors have a decay time that is much longer than the pulse duration, but much shorter than the pulse interval. This means that activator ions excited by a pulse all return to the ground state before the next pulse arrives. As the excitation density increases, the number of excited activator ions increases until all the activator ions are excited. The maximum averaged photon flux per unit phosphor volume is equal to the ratio of the activator concentration to the pulse interval. A high activator concentration is therefore required for linearity at high excitation densities. This largely explains why Tb^{3+} and Eu^{3+} phosphors with an activator concentration of 1-10% are far more linear than ZnS:Ag with an activator concentration of only 0.05% or less.

Further investigations showed, however, that this model is too simple. It does not explain the differences in linearity between various Tb^{3+} phosphors, for example. A more detailed analysis reveals that interactions between close activator ions in excited states initiate additional loss processes at high densities. The most direct proof of this is given by the luminescence decay [5], as shown in *fig. 5*. At low densities only the radiative decay of the activator is observed, but high densities give an initial shorter decay from which the additional loss can be derived. After some time the close activators that have been excited will have decayed, so that the slope again corresponds to the radiative decay.

The effect of interactions in excited states cannot be predicted very accurately, but must be determined experimentally. A general problem with measurements on projection-television tubes is the variation in the size of the electron spot with current. It is difficult to measure the spot size because of effects due to light scattering and sublinearity. A better control of the conditions can be obtained by measuring the luminescence output for short excitation pulses with a well-defined spot profile; we used a scanning electron microscope. The optical output can now be determined accurately as a function of the excitation density per pulse, given by $Vj\Delta t$, where V is the acceleration voltage, j the current density and Δt the pulse duration. At a fixed voltage, a curve of the output per pulse against $j\Delta t$ always has the same shape for a given phosphor, provided that Δt is much less than the initial decay time [6]. Although the values of j and Δt differ from the values in actual tubes, curves like the ones shown in fig. 4 can be used for comparing phosphors and predicting tube performance [7].

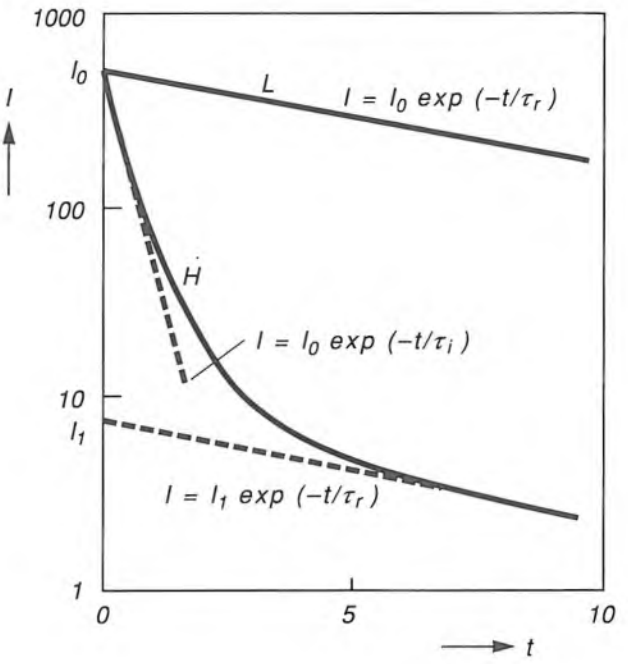

Fig. 5. Effect of the excitation density on the luminescence decay of a phosphor. The luminescence intensity I, on a logarithmic scale, is plotted against the time t, both in arbitrary units. The intensities at the end of the excitation pulses at $t = 0$ are set equal to I_0. A low-density pulse gives curve L: a straight line of slope $1/\tau_r$, where τ_r is the radiative decay time of the phosphor. A high-density pulse gives curve H, with an initial decay characterized by a slope $1/\tau_i$ followed by a tail with a slope $1/\tau_r$.

Comparisons of phosphors

In recent years many phosphors have been investigated in our laboratories to see if they would be suitable for application in projection-television tubes. The investigations combined the evaluation of well-known phosphors with a search for new phosphors. Data relating to the properties mentioned above will now be quoted for a number of phosphors.

Table I gives values for the energy-conversion efficiency and luminous efficacy at low excitation densities, the thermal quenching at 100 °C, the decay time and the sublinearity. The luminous efficacy is obtained by multiplying the energy-conversion efficiency by the lumen equivalent, i.e. the ratio of the number of lumens to the emitted power, calculated from the measured spectral distribution. The sublinearity can be conveniently characterized by two parameters: the relative efficiency at the average energy density per pulse, typically 10 mJ/cm^2 in present tubes, and the density at which the efficiency is half the efficiency in the linear regime.

The only phosphor we consider for blue is ZnS:Ag. Even though it is very sublinear it is still the only phosphor suitable for projection television, since there is no proven alternative. Its sublinearity is a great disadvantage in blending red, green and blue to produce white light, and the projection system has to be adapted to deal with this problem.

The green Tb^{3+} phosphors are much more linear than (Zn,Cd)S:Cu, and Y_2SiO_5:Tb and $Y_3(Ga,Al)_5O_{12}$:Tb are among the best. The choice of the Tb^{3+} phosphor also depends on the decay time, the available screen technology and the degradation with time.

[4] A. Bril, On the saturation of fluorescence with cathode-ray excitation, Physica **15**, 361-379, 1949;
A. Bril and F. A. Kröger, Saturation of fluorescence in television tubes, Philips Tech. Rev. **12**, 120-128, 1950.

[5] D. M. de Leeuw and G. W. 't Hooft, Method for the analysis of saturation effects of cathodoluminescence in phosphors; applied to Zn_2SiO_4:Mn and $Y_3Al_5O_{12}$:Tb, J. Lumin. **28**, 275-300, 1983.

[6] D. B. M. Klaassen, T. G. M. van Rijn and A. T. Vink, A universal description of the luminescence saturation behaviour per phosphor, J. Electrochem. Soc., **136**, 2732-2736, 1989.

[7] T. Doyle, D. B. M. Klaassen and M. J. G. Lammers, The influence of high scanning frequencies on the luminescence saturation properties of phosphors for CRT projection systems, IEEE Trans. **ED-36**, 1876-1881, 1989.

Table I. Comparison of blue-, green- and red-emitting phosphors for projection television. The Table shows the energy-conversion efficiency η_{CR} and luminous efficacy η_L for cathode-ray excitation at room temperature and low excitation densities, the ratio r_{th} of the efficiency at 100 °C to the efficiency at room temperature, the luminescence decay time τ, and the parameters characterizing the linearity at high excitation densities, i.e. the ratio r_{ex} of the efficiency at 10 mJ/cm² to the efficiency at low excitation densities, and $\varepsilon_{1/2}$, the excitation density at which the efficiency has been halved.

Phosphor	η_{CR}[a] (%)	η_L (lm/W)	r_{th}	τ (ms)	r_{ex}	$\varepsilon_{1/2}$ (mJ/cm²)
Blue						
ZnS:Ag	20	13	0.89	0.01-0.07[b]	0.23	2
Green						
(Zn,Cd)S:Cu	16	85	1.00	0.01-0.05[b]	0.12	2
$Y_3Al_5O_{12}$:Tb	8	35	1.00	3	0.61	20
$Y_3(Al,Ga)_5O_{12}$:Tb	9	42	0.97	3	0.82	70
Y_2SiO_5:Tb	9	41	0.94	2	0.88	95
LaOCl:Tb	10	45	0.98	1	0.70	25
$InBO_3$:Tb	8	42	1.00	7.5	0.76	45
Gd_2O_2S:Tb	11	48	0.80	0.7	0.51	10
Red						
Y_2O_2S:Eu	13	25	0.68	0.5	0.40	8
Y_2O_3:Eu	7	22	0.91	2	0.59	12

[a] Ratio of the luminescence energy output to the electron-energy input, of interest for practical tubes. If just the absorbed energy is considered higher values are obtained, since 10-20% of the incident electron energy is not absorbed because of back-scattering.
[b] Decreases with increasing excitation density.

Red phosphors include Y_2O_2S:Eu, used in direct-view tubes, and Y_2O_3:Eu. Although Y_2O_2S:Eu has a higher luminous efficacy at low densities, superior thermal properties and linearity make Y_2O_3:Eu the obvious choice for projection-television tubes.

The efficiencies and spectral data in the above comparisons represent intrinsic phosphor properties. However, to predict and assess the tube performance we also need to know the optical properties of phosphor layers in screens.

Optical properties of phosphor screens

Thin-film screens and powder screens have been considered for projection television. Thin-film phosphor screens are prepared directly on the substrate by deposition techniques such as epitaxy and evaporation. The screens are transparent and give excellent resolution and stability at high excitation densities. A major disadvantage, however, is their low photon escape in the forward direction due to internal light trapping and reflection and refraction losses at the interface with a medium of lower refractive index. Expensive substrates are also necessary: these have to be of single-crystal material for epitaxy, or unaffected by the high-temperature annealing required for vapour-deposited screens, for example. Thin-film screens have therefore been used mainly for professional applications where high resolution and contrast are required and the low efficiency can be compensated by high excitation densities.

Powder screens are preferred for consumer applications. These screens have to be prepared in two separate steps: the phosphor is prepared first and then deposited on the substrate. All thermal treatments at temperatures above 450 °C are carried out in the first step, so that less expensive substrates can be used. A characteristic feature of powder screens is multiple light scattering, which counteracts the decrease mentioned earlier in the photon escape and gives a forward gain in intensity instead. From now on we shall only consider powder screens.

The optical properties of a phosphor screen (*fig. 6*) are basically determined by the scattering and absorption in the powder layer and the reflectance of the aluminium film. It is not easy to formulate a theory for the light propagation, because of the complex topography and multiple scattering. Successful phenomenological calculations [8] have been restricted to one dimension and only give the output integrated over angle and position. We have developed a computer model for light propagation in three dimen-

sions [9]. The model gives complete information about the angular and spatial distribution of the light output and can be used for modelling the optical properties.

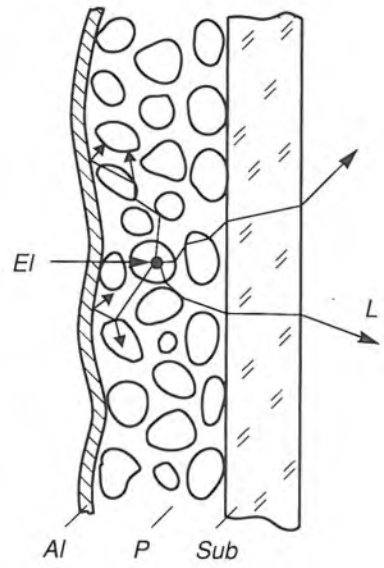

Fig. 6. Diagram of the cross-section of a phosphor screen for projection television. The phosphor is deposited as a powder layer *P* on a transparent substrate, typically a glass window a few mm thick. The layer is covered by a thin aluminium film *Al* (thickness 0.2 μm). Electrons *El* enter the phosphor layer from the aluminium side and the light generated *L* leaves the screen on the substrate side.

The model

The computer model is based on the continuum approximation using statistically distributed scattering and absorption centres with variable mean densities. Other input parameters are the layer thickness and the reflectance of the aluminium film. The effect of the substrate is neglected here, but the model has since been extended to include substrate effects such as the loss of contrast due to lateral light propagation ('halo effect') and the gain in forward intensity with interference filters [1].

In the simulations it is assumed that electrons with a typical penetration depth of 3 μm generate photons with an isotropic angular distribution. The propagation of the light is simulated by the Monte Carlo method: paths are traced for individual photons in the presence of the scattering and absorption centres. The probability of scattering is expressed by the mean pathlength between two scattering events; the angular probability is assumed to be isotropic. The probability of absorption is expressed by the mean pathlength of a photon before it is absorbed. Typical absorption lengths are larger than the scattering length by three orders of magnitude. Most photons therefore escape from the screen after several scattering events and reflections at the aluminium film. Although absorption in the phosphor only plays a minor part, it may become important after prolonged electron bombardment. Photons escaping from the screen are classified by position and angle of emergence.

Results

The emission intensity from a perfectly diffusing surface has a 'Lambert distribution': the intensity is proportional to the cosine of the angle θ between the normal to the surface and the direction of observation. The angular distribution from a phosphor powder screen, however, is affected by multiple scattering. *Fig. 7* shows the effect of different values of the scat-

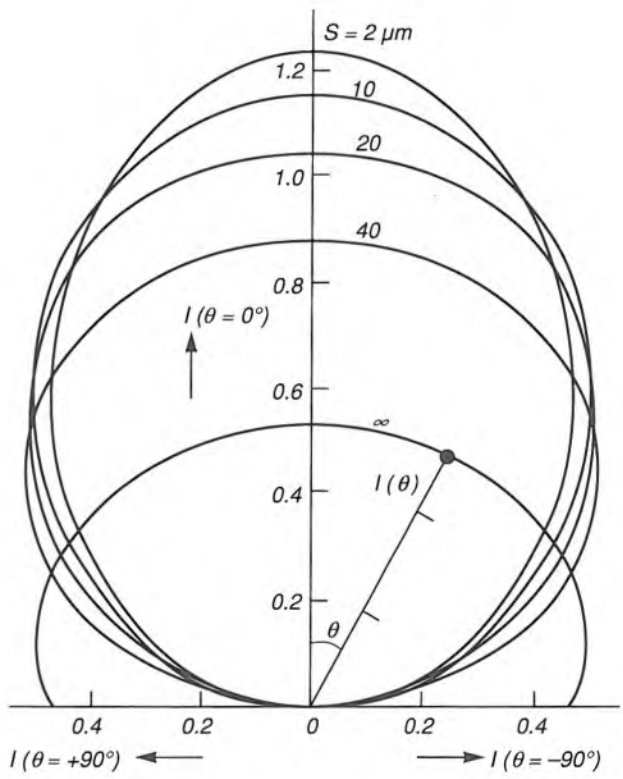

Fig. 7. Angular intensity distribution of a phosphor powder screen for cathode-ray excitation at five different values of the scattering length *S* and fixed values of the layer thickness (20 μm), absorption length (10 mm) and aluminium reflectance (90%). The intensity *I* is shown as a function of the angle θ to the normal, and its scale is normalized with respect to the Lambert distribution (see text). If the scattering is negligible (i.e. *S* is very large) the angular distribution is almost isotropic, with the effect of absorption visible at large angles. An increase in the scattering (i.e. a decrease in *S*) gives an increase in gain in the direction of the normal. At $S < 20$ μm, this gain is higher (up to 22%) than expected from the Lambert distribution.

[8] A. Bril and H. A. Klasens, Intrinsic efficiencies of phosphors under cathode-ray excitation, Philips Res. Rep. 7, 401-420, 1952.

[9] W. Busselt and R. Raue, Optimizing the optical properties of TV phosphor screens, J. Electrochem. Soc. 135, 764-771, 1988.

tering length S, with the intensity scale normalized to the Lambert distribution. At $S = 20\,\mu m$ the intensity in the forward direction ($\theta = 0°$) corresponds to the Lambert distribution. With increased scattering (smaller values of S) the intensity in the forward direction is larger: up to 22% at $S = 2\,\mu m$. If the scattering is negligible (very large S) the angular distribution is almost isotropic.

The optical performance of the phosphor screen depends on the amount of light emitted into the aperture of the projection optics. Increasing the scattering introduces two opposing effects, as shown in *fig. 8* for light emission within an acceptance angle of 50°. The forward gain in intensity gives an increase, whereas the angle-integrated output decreases because of the increased number of reflections at the aluminium film, which in turn leads to increased absorption losses and therefore to a lower photon-escape efficiency of the screen. As a result, the light output within the acceptance angle has a maximum at a scattering length of about half the layer thickness. Calculations with different screen parameters have shown that the optimum layer thickness is always about twice the scattering length. It was possible to show that this is the case if the layer thickness corresponds to about 2.5 times the mean grain size [9]. We should note, however, that this result only takes the optical properties into account. For optimum brightness the electron energy must be absorbed sufficiently. This means that there should be a minimum phosphor coverage for a given acceleration voltage.

As mentioned earlier, light scattering also affects the resolution. One measure of the loss of resolution is the line-spread function, i.e. the screen response to an infinitesimally narrow line. The calculated linewidth of the line-spread function at 5% of peak height increases linearly with layer thickness: see *fig. 9*. Calculations with varying scattering lengths, absorption lengths and aluminium reflectances have shown that these parameters have little effect. This has also been found experimentally for a wide range of screens with different phosphors, grain-size distributions and morphologies. Measured linewidths at 5% of peak height are also shown in fig. 9. To give a comparison with the calculated results we have also plotted the theoretical linewidth obtained when the finite resolution of the experimental arrangement is taken into account. The agreement between experimental and calculated linewidths confirms that the layer thickness is the dominant parameter; screens for high resolution should be as thin as possible. Screens with a sublinear phosphor such as ZnS:Ag have an additional loss of resolution at high excitation densities because of the associated increase in optical spot size [7].

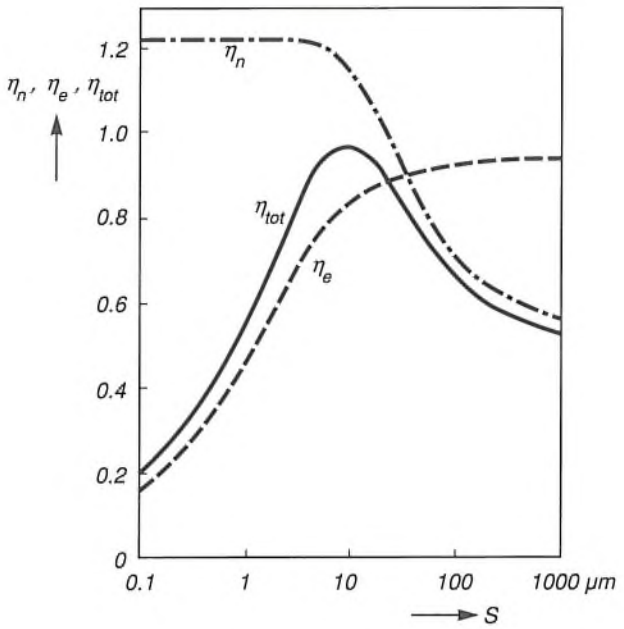

Fig. 8. Increasing the scattering (decreasing S) in a phosphor screen introduces two opposing effects on the amount of light emitted within a given acceptance angle (50°): the intensity with respect to the Lambert distribution (η_n) increases from about 0.5 to 1.22, whereas the angle-integrated screen efficiency (the photon-escape efficiency η_e of the screen) decreases because of the higher absorption losses. The resulting total screen efficiency η_{tot} has a maximum at $S \approx 10\,\mu m$.

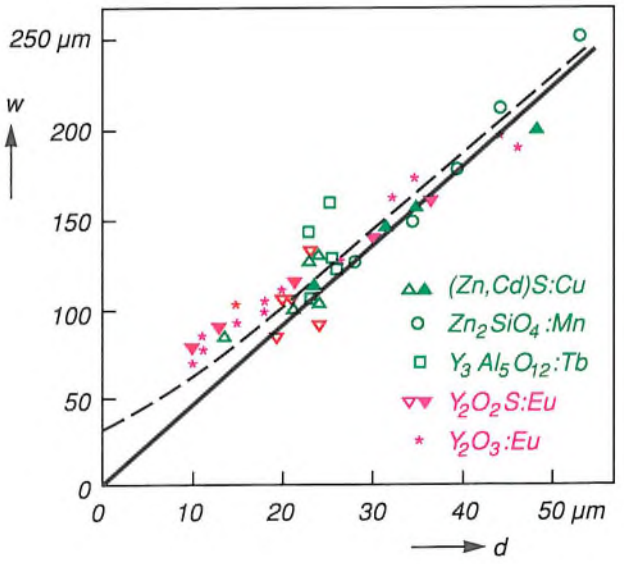

Fig. 9. Linewidth w of the line-spread function at 5% of the peak height, as a function of the layer thickness d of powder screens of several green-emitting and red-emitting phosphors with cathode-ray excitation. Some of the open circles represent results for different batches of the same powder varying in grain size; the lower linewidths correspond to smaller grains for a given layer thickness. Calculated curves are also shown (see text); in the upper curve the broadening due to the experimental arrangement has been taken into account. The agreement between experiment and theory is good; this proves that the linewidth is mainly determined by the layer thickness.

Screen processing

In screen processing it is important to be able to produce a thin layer. For an electron penetration depth of 3 μm and a maximum phosphor packing density of 60%, the minimum thickness should be about 5 μm. Since the average thickness of an optimum screen is about 2.5 grains, the minimum grain size should be about 2 μm. However, it is not easy to prepare such small grains with a high luminescence efficiency and a good yield, and they are difficult to handle in screen processing. This means that larger grains are often preferred, but here again there is a maximum, determined by the loss of resolution with increasing grain size and screen thickness. In the tubes now manufactured for the consumer market the mean grain sizes range up to about 10 μm. The size distribution should be narrowly centred around the mean grain size for a homogeneous screen.

The morphology of the grains is also important. Since the phosphor must be stable at high excitation densities, small single crystals are preferred. They should be simple in shape to permit close packing. The grains must also be chemically stable so that they are not affected by the screen processing. This is usually carried out in an aqueous basic or acid environment, and requires heat treatments at up to 450 °C.

In screen preparation a phosphor layer and a high-reflectance aluminium film must be deposited. The aluminium film is usually vapour-deposited on a polymer film previously applied to the phosphor layer. This prevents the aluminium from penetrating the phosphor, which would cause severe optical absorption. After the aluminium deposition the polymer film is removed by baking the screen.

Both wet and dry processes can be used for depositing the phosphor layer. In dry processes the substrate is first coated with adhesive, and the phosphor powder is dusted on to the adhesive coating. The powder may be mechanically mixed with the adhesive to improve layer homogeneity and adhesion. Photosensitive adhesives can also be used. With an appropriate binder, the powder can be processed to form a paste that can be printed on to the substrate directly (screen printing). In wet processes a phosphor suspension with a dispersing agent is prepared. This suspension can be added to a bath with the substrate at the bottom; the phosphor grains sink to the substrate where the powder layer is formed (sedimentation). If the grains are charged, the deposition can be induced by an electric field (electrophoresis). Suspension can also be spread over the substrate by tilting and rotating (flow coating). In all processes a binding agent must be used, either in the bath or on the substrate.

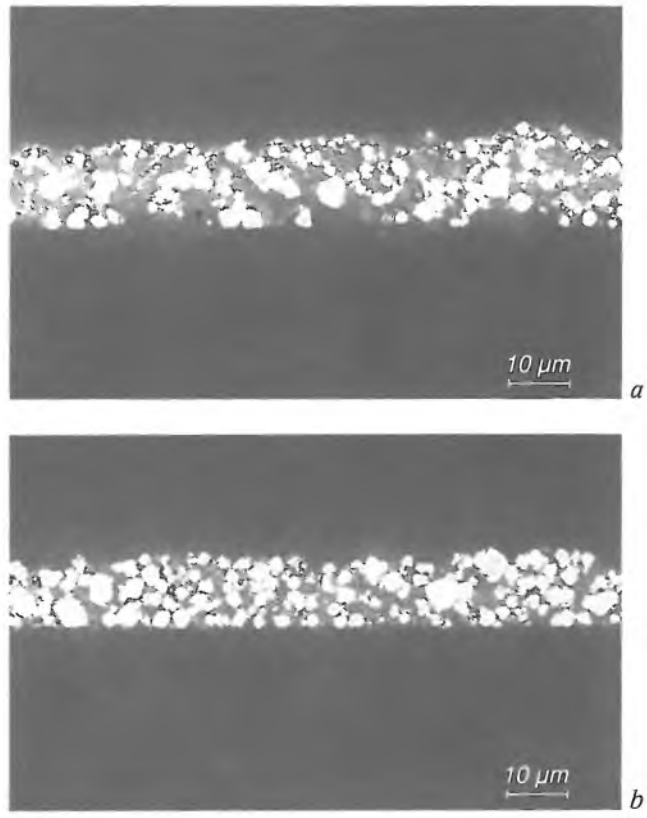

Fig. 10. Cross-sectional view of powder screens containing Y_2O_3:Eu, prepared by a standard process (*a*) and by an improved process (*b*) giving a much higher packing density.

The most important process for the preparation of screens for projection television is sedimentation. This is a simple technique and gives screens with good brightness, resolution and operating life. The renewed interest in screens for high-definition television (HDTV) has led to some modifications in the process to give improved resolution and life but without loss of brightness.

The sedimentation process is characterized by geometrical parameters such as the height of the liquid in the sedimentation bath, and also by the binder chemistry, which has a considerable influence on the final screen performance and the chemical stability under electron excitation. In a preferred process the phosphor grains are dispersed in a silicate solution that forms part of the binder system and also gives the grains a negative charge and prevents them from sticking together ('agglomeration'). The suspension is poured into the sedimentation vessel with an aqueous electrolyte to act as the coagulant. The positive ions in the electrolyte induce binding between the charged grains and between the grains and the substrate.

The screen structure can be affected by the composition and pH-value of the dispersion solution and the sedimentation bath. *Fig. 10* shows cross-sections

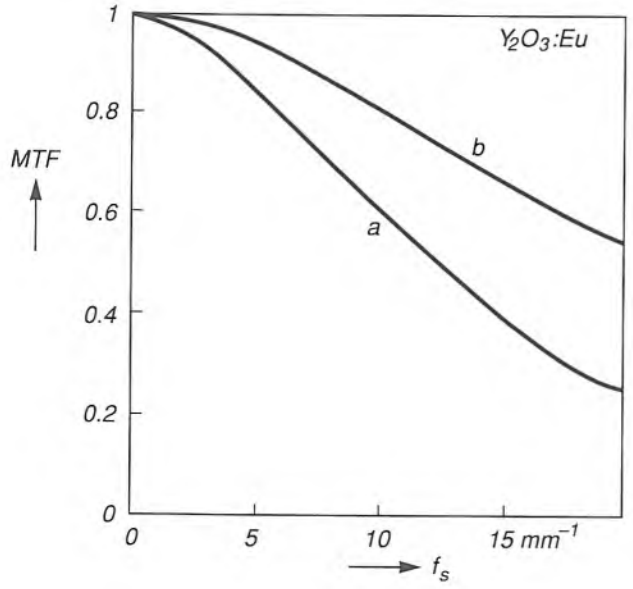

Fig. 11. Resolution as expressed by the modulation transfer function *MTF* plotted against the spatial frequency f_s, for the two screens of fig. 10. The screen with the high packing density (*b*) gives a much better resolution than the one with the low packing density (*a*).

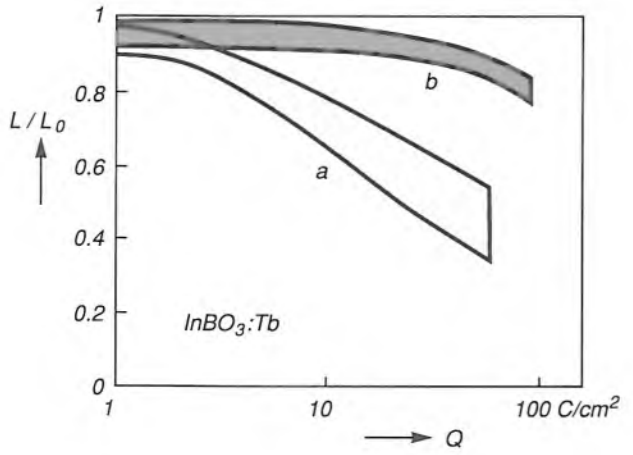

Fig. 12. Effect of the screen processing on the degradation of the light output of a large number of $InBO_3$:Tb powder screens. The ratio of the light outputs after ageing and before ageing (L/L_0) is plotted against the total charge deposited per unit area (Q), a measure of the operating life. Screens prepared by an improved process giving a high packing density (*b*) degrade more slowly than the screens prepared by a standard process (*a*).

of two screens containing Y_2O_3:Eu prepared under different conditions. The screen obtained by a standard process has a packing density of between 30% and 40%. An improved process using a buffering electrolyte gives a screen with a packing density of up to 60%. For a given weight this screen gives a much better resolution, because the layer is thinner. This is shown in *fig. 11*, where the resolution of the two screens is shown as a plot of the modulation transfer function against the spatial frequency.

Preparation processes giving higher packing densities also improve the life. This is shown in *fig. 12*, where the light output is plotted against the electron charge deposited for a large number of $InBO_3$:Tb screens. A similar improvement has been observed for screens with other phosphors. This has not yet been completely explained, but we can point to two significant factors. One is the low probability of electrons passing through a high-density phosphor layer, so that fewer electrons penetrate the glass substrate to give browning of the glass. The other is related to the difference in binder content. In the standard process, binding is induced by a colloidal silicate, whereas in the improved process the phosphor grains are coated with a dense vitreous silicate layer that stabilizes the phosphor to prevent electron damage. We shall now consider the degradation in more detail.

Degradation

Degradation, i.e. the decrease in light output under prolonged electron bombardment, depends on the phosphor properties, the screen processing and the tube processing. A good way of investigating degradation is by carrying out ageing experiments on actual tubes. We can predict the performance in practical conditions from these experiments, and further analysis on aged tubes will provide a better understanding of the main causes of degradation.

Ageing experiments

Most phosphor screens are subject to 'Coulomb ageing', which means that the decrease in light output at a fixed acceleration voltage depends only on the deposited charge per unit area. An example of such behaviour is shown in *fig. 13a* for ZnS:Ag. In this case it is easy to predict the tube performance for different operating conditions and to perform accelerated life tests.

With some phosphors, however, we observe a non-Coulomb ageing: their degradation also depends on the current density during ageing, as shown in fig. 13*b* for LaOBr:Tb. This complicates the testing of new phosphors and screen processes. A staircase video pattern dividing the phosphor screen into regions, each aged with a different beam current, has therefore been employed [10]. This means that the effect of different beam-current densities on a tube can be studied, and the aged screen can also be used for further analysis of the regions that have received different Coulomb doses. Changes in luminescence and optical properties can be measured at regular time intervals during ageing, or they can be measured in different regions after ageing.

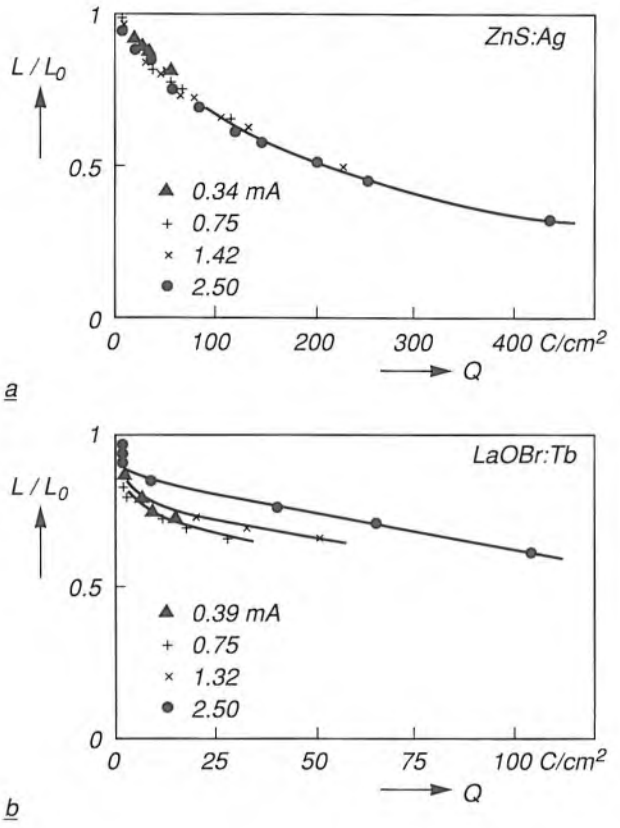

Fig. 13. Relative light output L/L_0 of two types of phosphor screen as a function of the charge deposited per unit area (Q) at different values of the beam current during ageing. The degradation of the light output is independent of the beam current for ZnS:Ag screens (*a*), but does depend on it for LaOBr:Tb screens (*b*).

Degradation mechanisms

In discussing possible mechanisms for the decrease in luminous efficacy of the phosphor screen we shall again consider the various stages in the energy-conversion process; see fig. 3 and eq. (1). The parameters sensitive to ageing are the efficiency of the energy transfer from the phosphor host lattice to the activator, the quantum efficiency of the activator luminescence and the photon-escape efficiency of the screen.

The transfer efficiency η_t, can be decreased by generating killer centres in the bulk or at the surface. The presence of these centres can be observed as an increased linearity at high excitation densities. The transfer efficiency can also be decreased by reducing the concentration of effective luminescent centres, which will reduce the light output at high excitation densities [11].

The quantum efficiency η_a of the activator luminescence can be decreased by an increase in the non-radiative loss processes in the activator due to the electron bombardment. The most direct proof of the existence of these processes can be seen in a reduction in the luminescence decay [11].

A decrease in η_t and η_a can also be demonstrated by comparing the light output of aged and non-aged screens as a function of the acceleration voltage. After ageing, a lower output at low voltages (and hence a

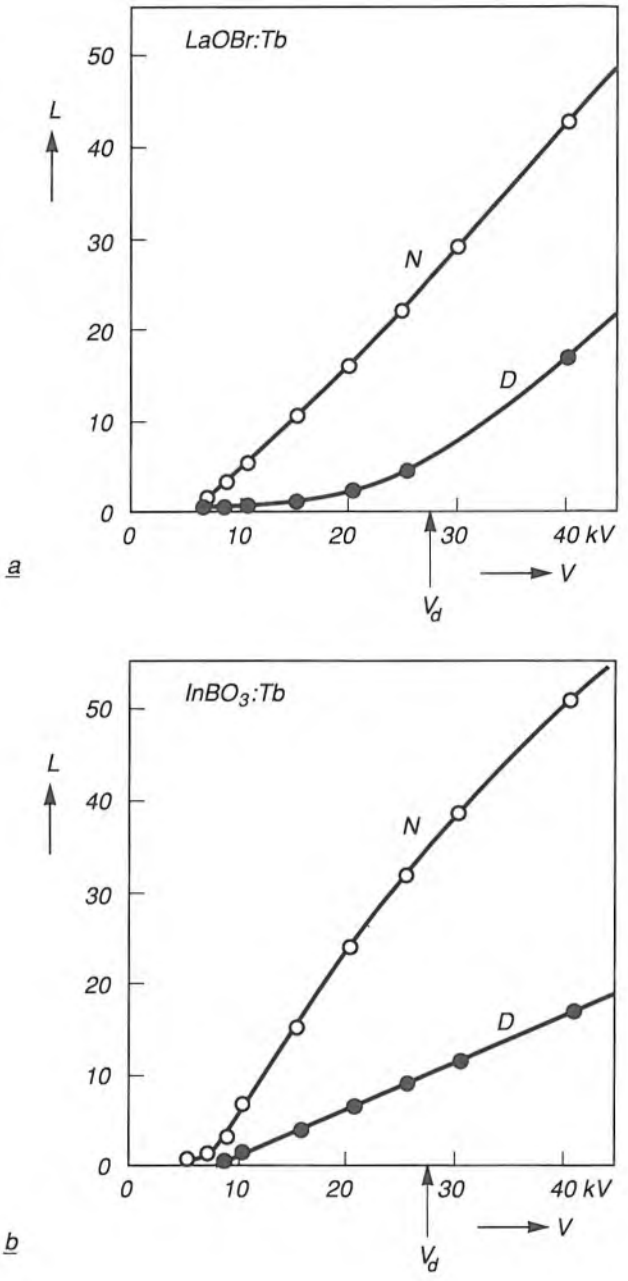

Fig. 14. Light output L (in arbitrary units) measured as a function of the acceleration voltage V for LaOBr:Tb screens (*a*) and $InBO_3$:Tb screens (*b*), non-degraded (N) and degraded (D) at a fixed voltage V_d. In the non-degraded screens the light output increases much more rapidly with voltage. In degraded LaOBr:Tb screens there is a superlinear increase at voltages above V_d.

[10] T. Welker, S. Klauer, J. H. M. Spruit and L. Vriens, Aging of phosphors in projection TV tubes, Extended Abstracts Electrochem. Soc. **87-2** (Fall Meeting, Honolulu, Hawaii, 1987), pp. 1730-1731.

[11] D. B. M. Klaassen, D. M. de Leeuw and T. Welker, Degradation of phosphors under cathode-ray excitation, J. Lumin. **37**, 21-28, 1987.

low electron penetration depth) indicates an increase in surface losses. The effect of bulk deterioration on η_t and η_a is revealed by a superlinear increase in the output at higher voltages when the primary electrons excite a non-aged region. Such an increase has been observed in LaOBr:Tb, for example, but not in $InBO_3$:Tb; see *fig. 14*.

The photon-escape efficiency η_e of the screen depends on the scattering and absorption in the phosphor layer, the reflectance of the aluminium film and the thickness of the phosphor layer. A significant effect that may arise with electron bombardment is an increase in the absorption in the phosphor layer, giving a reduction in η_e. There may also be browning of the glass faceplate; this increases its diffuse reflectance and decreases its transmittance, which also gives a reduction in η_e. The change in η_e can be calculated by the Monte Carlo method from the measured reflectance of the screen and the reflectance and transmittance of the uncoated faceplate.

Analysis of aged screens

A variety of aged screens have been investigated to find the dominant degradation mechanism for various phosphors. We have used the results of the optical measurements to calculate the values of η_e. In *fig. 15* η_e is plotted as a function of the light output, both normalized to the values determined for non-aged screens. The points on the straight line correspond to degradation due entirely to a decrease in η_e. This is the case for ZnS:Ag, LaOCl:Tm, $InBO_3$:Tb and Y_2O_3:Eu, but not for LaOBr:Tb and Y_2SiO_5:Tb, in which the decrease in η_e is much less than the decrease in light output. In these phosphors a decrease in η_t or η_a, or in both of them, must be the main reason for the deterioration. As would be expected, the variation in their light output as a function of the acceleration voltage gives a superlinear increase at high voltages, as was shown in fig. 14 for LaOBr:Tb. This gives further evidence of a deterioration in the generation of light (η_t and η_a), since η_e is not very dependent on the position at which the light is generated. We have also observed that these phosphors are more linear after ageing, which indicates that killer centres are formed in the bulk, so that the transfer efficiency is reduced.

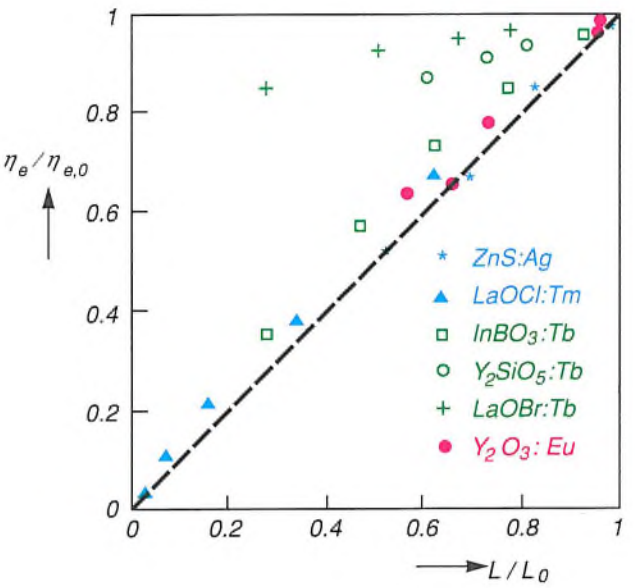

Fig. 15. Calculated values of the relative photon-escape efficiency $\eta_e/\eta_{e,0}$ plotted against the relative light output L/L_0 of various phosphor screens at different stages of degradation. For ZnS:Ag, LaOCl:Tm, $InBO_3$:Tb and Y_2O_3:Eu the decrease in light output is closely related to the decrease in the escape efficiency. For Y_2SiO_5:Tb and LaOBr:Tb, however, the light output decreases more rapidly than the escape efficiency.

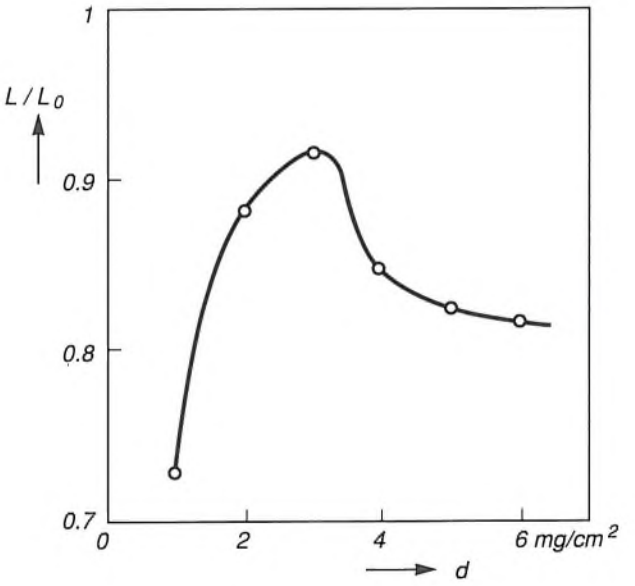

Fig. 16. Typical curve for the relative light output L/L_0 of deteriorated screens as a function of the screen weight per unit area (d). A charge of 100 C/cm^2 was deposited during ageing. Increasing the screen weight first gives a higher light output, but as the weight increases the light output decreases.

Improvement of the degradation behaviour

In phosphor screens whose degradation is dominated by a decrease in the photon escape efficiency there are usually only negligible changes in the luminescence properties. This indicates that increased absorption in the bulk material is unlikely for these 'absorption-deteriorated' phosphors. The absorption is more likely to take place on the surface of the grains, in the binder of the screen or in the browned glass faceplate. The degradation can therefore be reduced by improving the screen processing, as has been demonstrated for screens containing $InBO_3$:Tb (fig. 12).

The degradation of absorption-deteriorated phosphors has been found to depend closely on the screen

weight. A typical example is shown in *fig. 16*, where the relative light output of aged screens is plotted against the screen weight. The increased degradation at low weights can be ascribed to an increased glass browning due to electrons unabsorbed by the phosphor layer. At high screen weights, the degradation increases because of the longer path of the photons before leaving the screen. An increasing degradation due to a larger effective photon pathlength also occurs when these phosphors are combined with interference filters [1].

A different approach is necessary for 'intrinsic-deteriorated' phosphors such as LaOBr:Tb and Y_2SiO_5:Tb where the reduction in η_t and η_a is dominant (fig. 15). An improvement in their degradation behaviour should start with an optimization of the phosphor powder itself. These phosphors are however of interest for use in combination with interference filters, because their degradation is not affected by an increase of the effective photon pathlength.

Outlook

Many aspects of phosphor screens for projection television are now well understood. This is particularly useful for predicting their behaviour in future high-quality large-screen projection systems, in which the improvements will include better resolution, higher luminance and the absence of noise and flicker. It will also be easier to identify any problems that may be associated with such improvements. The use of interference filters between the phosphor layer and the faceplate [1] can also be taken into account in such predictions; one application of these filters is for adjusting non-ideal chromaticities of new or existing phosphors [12].

A problem at present is that ZnS:Ag is highly sublinear. However, there is as yet no fully proven alternative blue-emitting phosphor to compete with ZnS:Ag, even with chromaticity correction from interference filters. The most promising activators from the rare-earth ions are Tm^{3+}, which gives a line emission around 460 nm, and Ce^{3+}, which gives a blue band emission in suitable host lattices. The best Tm^{3+} phosphor for projection television is probably La(Ga,Al)O_3:Tm, but its efficacy only approaches that of ZnS:Ag at excitation densities higher than those used in present projection tubes [13]. A phosphor that can compete with ZnS:Ag at the high densities used in present tubes is (La,Gd)OBr:Ce. However, this phosphor requires a special screen-making process because it is sensitive to water [14]. The plate-like morphology of the phosphor crystallites also has adverse effects on the photon escape efficiency. Further effort is therefore required if the full potential of these phosphors is to be exploited.

ZnS:Ag can be retained and the effect of sublinearity can be diminished if the excitation density per pulse is reduced. This can be done by defocusing the electron spot slightly; the defocusing is hardly visible in the picture because the blue resolution of the eye is limited. However, future improvements in picture resolution will require a smaller spot size for blue. A better way of decreasing the excitation density per pulse without losing resolution is to increase the scanning frequency. Quadrupling the scanning frequency would reduce the excitation density per pulse by the same factor, giving much improved linearity for the light output from the tube [7].

The contribution from the green emission to the luminous output in the white of the picture amounts to about 70%. Improvements in the green-emitting phosphors are therefore always important. A green-emitting phosphor that is also efficient at high densities is LaOBr:Tb, with a luminous efficacy approaching 60 lm/W. However, this phosphor gives much the same problems in screen processing as (La,Gd)OBr:Ce, since it is sensitive to water and has a plate-like grain morphology; further research is required.

It seems unlikely that a replacement for Y_2O_3:Eu as a red emitter will be required in the near future.

The degradation in light output of phosphor screens for projection television is another important area for further research. We have seen that the degradation behaviour of many screens is also related to screen technology, not just to intrinsic phosphor properties. We expect further research to give further significant improvements in degradation behaviour.

[12] D. B. M. Klaassen, D. M. de Leeuw and C. A. H. A. Mutsaers, Projection cathode-ray tubes comprising blue emitting phosphors with interference filters, J. Electrochem. Soc. **136**, 858-862, 1989.

[13] K. J. B. M. Nieuwesteeg and C. A. H. A. Mutsaers, Preparation and characterization of thulium-activated La(Al,Ga)O_3 phosphors for blue-emitting cathode ray tubes, Philips J. Res. **44**, 157-182, 1989.

[14] D. M. de Leeuw, C. A. H. A. Mutsaers, H. Mulder and D. B. M. Klaassen, Blue emitting phosphors for projection cathode ray tubes, (La,Y)OBr:Ce and (La,Gd)OBr:Ce, J. Electrochem. Soc. **135**, 1009-1014, 1988.

Summary. Phosphor screens in tubes for projection television have to meet some critical requirements, since they operate at much higher electron-excitation densities than the screens in conventional direct-view tubes. Their light output should be only slightly sublinear at high excitation densities and should be stable under prolonged intense electron bombardment. This affects the selection of the phosphors and the screen processing. The preparation of screens with the optimum light output and resolution requires a careful evaluation of their optical properties and degradation behaviour.

Philips Tech. Rev. 44, No. 11/12, 348-356, Nov. 1989

Electron guns for projection television

T. G. Spanjer, A. A. van Gorkum and W. M. van Alphen

While the previous article was about phosphors in cathode-ray tubes for projection television, the article below is about the electron guns that excite the phosphors. As in conventional tubes for direct-view television, these guns contain a cathode for electron supply and a number of electron-optical lenses that form the electron beam and focus it on the phosphor screen. To produce the sharp bright images required for projection television, the beam must have a high intensity and a very small diameter at the point where it meets the screen. This sets difficult requirements on the design of the electron guns.

Introduction

The electron gun in a cathode-ray tube for television produces an electron beam that excites the phosphor layer (the 'phosphor screen') on the faceplate of the tube, causing it to emit light. In direct-view colour television this screen contains three different phosphors that emit light in the primary colours red, green and blue, and the viewer looks directly at the picture on the faceplate of the tube. In projection television three small cathode-ray tubes provide separate images in red, green and blue. These images are magnified about 10 times and superimposed on a large projection screen. The pictures should be comparable in brightness and resolution with direct-view television. This requires electron guns that provide a much smaller electron spot at the screen than in conventional cathode-ray tubes. Phosphors are also required with a high light output, which is still reasonably linear with beam current even at high current densities.

In the last few years there has been greatly increased interest in projection television, mainly because improvements in various components have given much better picture quality. A further stimulus to the application of projection television will be the introduction of high-definition television (HDTV) with large screens.

Dr Ir T. G. Spanjer, Dr Ir A. A. van Gorkum and Dr W. M. van Alphen are with Philips Research Laboratories, Eindhoven.

In an earlier article in this journal [1] it was shown how the brightness, colour rendering and resolution of projection television can be improved by applying interference filters to the faceplates of the three tubes and by using curved faceplates in the tubes. We have already considered the behaviour of phosphors in the previous article [2]; now we shall consider the electron guns.

The principle of a cathode-ray tube for television and the operation of an electron gun are illustrated in the diagram of *fig. 1*. The triode of the gun emits a divergent electron beam whose intensity at any instant is proportional to the brightness of the pixel to be reproduced. The beam is focused by an electron-optical lens (the 'main lens'), consisting of regions with differing electric (or magnetic) fields, to produce a small 'electron spot' at the phosphor screen. Between the gun and the screen the beam is deflected by two time-dependent magnetic fields to 'write' the image on the phosphor screen. The intensity of the light emitted is determined by the beam current and the luminescence properties of the phosphor layer. The resolution is determined by the size of the electron spot and the light scattering in the phosphor layer.

The tubes used for projection television are small, with a typical usable screen diagonal of 125 mm. To obtain sufficiently bright pictures at the phosphor

screen, the beam current should be high, up to about 6 mA. To give the required resolution, the electron spot should have a diameter no more than a few tenths of a millimetre, much smaller than for conventional direct-view tubes at about the same current (a few millimetres).

The objective of the study described in this article was the design of electron guns that would meet these requirements. One difficulty in reducing the size of the spot is that of aberrations in focusing the beam on to the screen. These arise because the electrons — or 'electron rays' — at the outside of the beam are deflected too strongly ('spherical aberration'). These errors make a significant contribution to the size of the spot on the screen. The effect of spherical aberration can of course be reduced by reducing the beam diameter in the main lens by using a prefocusing lens, but the improvement is insufficient for high-definition projection television.

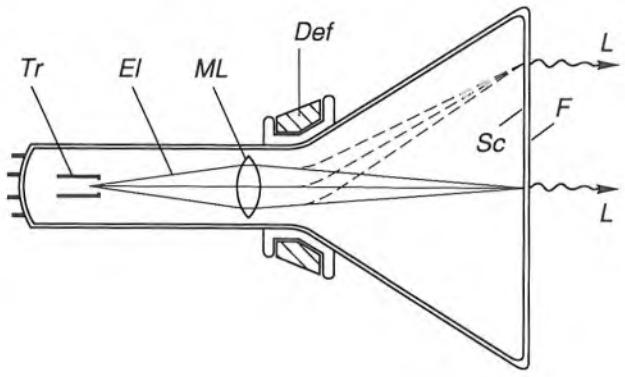

Fig. 1. Principle of a cathode-ray tube for television. The electron gun in this tube consists of a triode *Tr* that gives a divergent electron beam *El*, and a main lens *ML* that focuses the beam on to the phosphor layer of the screen *Sc*. Time-dependent magnetic fields from the deflection coil *Def* deflect the beam in two directions, so that the image is 'written' on the screen. The electrons that strike the phosphor layer excite light *L*, which emerges via the faceplate *F* of the tube.

After calculating the electron trajectories and the spot size in various kinds of gun, we have been able to derive a new design. This is based on a triode with an impregnated cathode that permits higher beam loading and therefore a more intense beam than a conventional oxide cathode [3]. Another improvement relates to the main lens: the conventional electrostatic lens, formed by electrodes at different potentials, has been replaced by an electromagnetic lens, formed by a coil around the neck of the tube. This has the advantage that the lens diameter can be larger for given tube dimensions, so that the spherical aberration is reduced [4].

However, the greatest improvement is obtained by adding two extra electrodes to form a *selective* prefocusing lens. The advantage of using such a lens, also known as an aberration reducing triode, or ART, had already been demonstrated earlier in calculations of the spot size [5] and in applications in other electron guns [6]. This lens is positioned so that well before the main lens the electron rays at the outside of the beam are interchanged with rays inside the beam. It considerably reduces the total spherical aberration and gives a more uniform intensity distribution in the beam. This results in a much smaller electron spot.

The new design has been optimized with the aid of electron-optical calculations and measurements. Guns and tubes of this design have been made and the characteristics relevant to projection television have been investigated. We have found that a spot diameter of 0.185 mm can be obtained at a beam current of 4 mA. This means that the brightness and resolution meet the requirements for high-definition projection television.

In this article we shall first look more closely at the resolution of electron guns, and at possible ways of improving them. We shall then give some details of the new electron-optical design and the construction of the gun and tubes. Finally, the most important results from the measurements will be discussed.

The resolution of electron guns

Limitations of the triode

The general configuration and operation of a triode in an electron gun are shown schematically in *fig. 2*. A planar cathode emits electrons under the influence of the accelerating electric field of an electrode at a positive potential with respect to the cathode. An intermediate electrode at a low negative potential provides a decelerating electric field, which confines the electron emission to the central part of the cathode. The electrons are deflected towards the axis of the

[1] L. Vriens, J. A. Clarke and J. H. M. Spruit, Interference filters for projection television tubes, Philips Tech. Rev. **44**, 201-210, 1989.

[2] R. Raue, A. T. Vink and T. Welker, Phosphor screens in cathode-ray tubes for projection television, this issue, pp. 335-347.

[3] J. Hasker, J. E. Crombeen and P. A. M. van Dorst, Comment on progress in scandate cathodes, IEEE Trans. **ED-36**, 215-219, 1989.

[4] A. A. van Gorkum and T. G. Spanjer, A generalized comparison of spherical aberration of magnetic and electrostatic electron lenses, Optik **72**, 134-136, 1986.

[5] A. A. van Gorkum and M. H. L. M. van den Broek, Spot reduction in electron guns using a selective prefocusing lens, J. Appl. Phys. **58**, 2902-2908, 1985.

[6] S. Ashizaki, Y. Suzuki, O. Konosu and O. Adachi, 43-inch direct-view color CRT, Jap. Display 1986, pp. 226-229;
J. Gerritsen and P. G. J. Barten, An electron gun design for flat square 110° color picture tubes, Proc. SID **28**, 15-19, 1987.

rotationally symmetric field, thus producing a 'crossover'. The electric field that produces this convergence is called the cathode lens. After the electrons have passed the crossover, they diverge until they reach the main lens, which produces an image of the crossover on the phosphor screen.

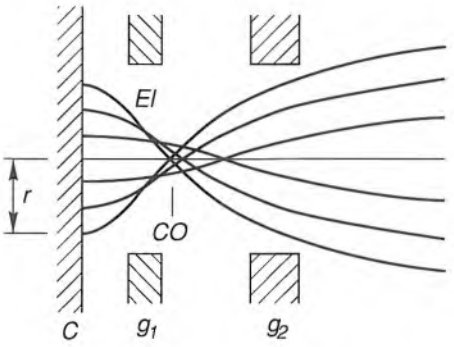

Fig. 2. Schematic geometry and operation of a triode in an electron gun. Electrons *El* emerge from the surface of the cathode *C*. The electrode g_1 has a low negative potential with respect to the cathode, so that the electrons are decelerated and the emission remains limited to an area of radius *r*. Because of the presence of the electrode g_2, which has a high positive potential, a 'crossover' *CO* is produced close to g_1.

In the ideal case the crossover would be a point. But in practice there are aberrations, which means that the crossover occupies a region around the axis (fig. 2). The most important contribution to the increase in the magnitude of the crossover comes from the spherical aberration of the cathode lens: electrons emerging from the cathode further away from the axis will cross the axis closer to the cathode than electrons starting closer to the axis. Another effect is that the electrons do not all leave the cathode along a normal: the angle of emergence can have any value between 0 and 90° because of the thermal spread in the transverse velocities of the electrons. The contribution from this effect to the size of the crossover depends on the cathode temperature, the type of cathode and the beam current. A third effect is the 'space-charge effect': the electron concentration at the crossover is associated with a strong interaction between the electrons, in which they tend to repel one another. This effect increases with the beam current.

It is not easy to quantify the individual contributions from each of these three effects, since they are all correlated. Nevertheless, it is clear that they degrade the resolution appreciably. The final resolution is degraded even further by focusing errors at the phosphor screen originating from spherical aberration in the main lens.

Spherical aberration of various main lenses

Various kinds of main lens can be used for imaging the crossover on the phosphor screen. We have made calculations to compare the spherical aberration in three different types, one electromagnetic, the other two electrostatic. It was assumed in the calculations that the brightness was constant at the crossover and that the beam diameter in the main lens had the optimum value. We expressed the spherical aberration in terms of three characteristic geometrical parameters. The first parameter is the distance *P* from the centre of the lens to the crossover. This distance, approximately equal to the length of the electron gun, is one of the factors that determine the length of the tube and is therefore a critical parameter. The second parameter is the distance *Q* from the centre of the lens to the phosphor screen, which depends on the screen dimensions and the deflection angle. The third parameter is the lens diameter *D*, which in practice is mainly determined by the diameter of the neck of the tube.

A diagram of the lenses that we have studied is given in *fig. 3*. In the electromagnetic lens the magnetic field is produced by a coil inside a cylindrical iron yoke. The yoke has an internal diameter of *D* and a gap of width 0.1 *D*. One of the electrostatic lenses is a 'bipotential lens' formed by two cylindrical electrodes, with the same diameter *D* and a gap width of

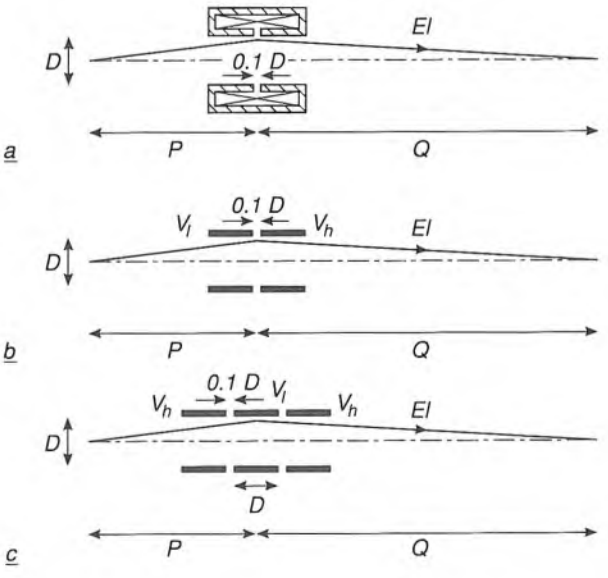

Fig. 3. Geometry of three types of focusing lens for which the spherical aberration has been compared. The important parameters are the lens diameter *D* and the distances *P* from the centre of the lens to the crossover and *Q* from the centre of the lens to the screen. *a*) Electromagnetic lens formed by a coil in a cylindrical yoke. *b*) Electrostatic bipotential lens formed by two cylindrical electrodes, one at a low potential V_l and the other at a high potential V_h. *c*) Electrostatic unipotential lens formed by three cylindrical electrodes, with the central lens at a potential V_l and the others at a higher potential V_h.

0.1 D, but at different potentials. The other lens is a 'unipotential lens' formed by three cylindrical electrodes of diameter D and gap widths 0.1 D, with the two outer electrodes at the same high potential and the central electrode, of length D, at a lower potential.

The calculations were performed for guns with P between 50 and 100 mm and Q between 150 and 210 mm, typical values for projection-television tubes. Diameters between 18 and 36 mm were used for the electromagnetic lens in the calculations, and diameters between 12 and 30 mm for the electrostatic lenses. We calculated the quantity $C^{1/4}$ as a measure of the spherical aberration, where C is the aberration coefficient [4]. The value of $C^{1/4}$ is proportional to the smallest spot diameter that can be obtained with the optimum beam diameter in the main lens, at a given brightness of the beam emerging from the triode.

In *fig. 4* the quantity $C^{1/4}$ is plotted against P for Q-values of 150 and 210 mm and a lens diameter of 30 mm. This figure shows that the spherical aberration is much the same for each of the three types of lens. It can also be seen that increasing P has little effect: a slight reduction of the spherical aberration. A change in Q has a greater effect: for all three kinds of lens the spherical aberration is much larger for $Q = 210$ mm than for $Q = 150$ mm.

The calculations also show that $C^{1/4}$ is proportional to $D^{-1/2}$. An electromagnetic lens has definite advantages for reducing the spherical aberration by increasing the lens diameter: since the magnetic field is produced outside the neck of the tube, the diameter can be larger for the same tube dimensions than with an electrostatic lens. The results described here were used in optimizing the new electron-optical design.

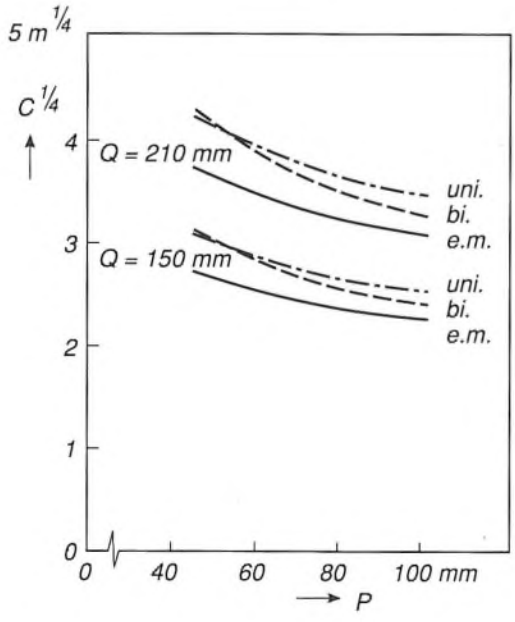

Fig. 4. Calculated value of $C^{1/4}$, a measure of the spherical aberration, as a function of P at two values of Q for the three lenses of fig. 3 with $D = 30$ mm. The electromagnetic lens gives the lowest spherical aberration, but the difference from the other lenses is not particularly great. The effect of Q is larger than that of P.

Improvement by selective prefocusing

To reduce spherical aberration in the focusing action of the main lens a prefocusing lens is often used. This lens is inserted between the crossover and the main lens, so that the beam diameter at the main lens is reduced. The prefocusing lens is usually located some way from the crossover; see *fig. 5a*. The prefocusing

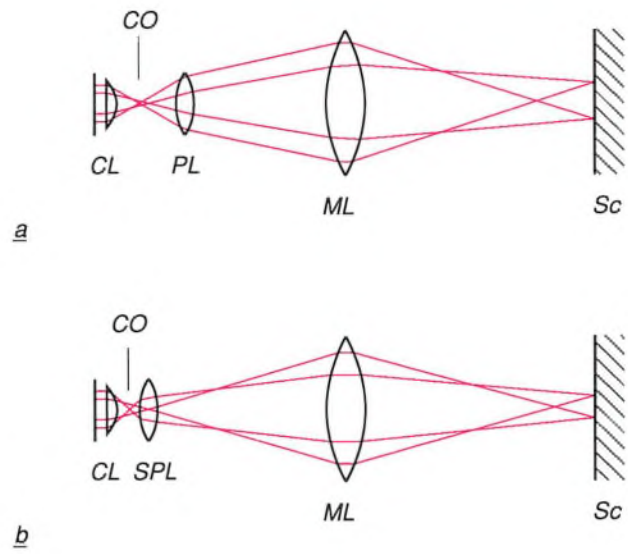

Fig. 5. Effect of the spherical aberration in an electron gun with a conventional prefocusing lens *PL* between the crossover *CO* of the cathode lens *CL* and the main lens *ML* (*a*), and with a strong selective prefocusing lens *SPL* (or aberration-reducing triode, ART) close to the crossover (*b*). The selective prefocusing forces the outer rays of the beam inwards. This gives a smaller electron spot on the screen *Sc* when the beam is focused by the main lens, and a more uniform intensity distribution in the beam.

lens performs an integral converging action on all the rays in the beam. The spherical aberrations of the cathode lens and the main lens are usually additive, because the outer rays at the cathode remain on the outside of the electron beam throughout the entire gun. The result is that the spherical aberration is too high for satisfactory application in high-definition projection television, particularly at high beam currents.

A considerable improvement is obtained if the prefocusing lens is made stronger and placed much closer to the crossover; see fig. 5*b*. The outer rays, which cross the axis some way away from the crossover, are then much more strongly refracted, while the inner rays are hardly refracted at all. This selective prefocusing interchanges the inner and outer rays, so that

the spherical aberrations of the cathode lens and the main lens are no longer additive. The result is a very considerable reduction in the total spherical aberration and therefore a much smaller electron spot.

Calculations of the spot diameter show that the effect of the selective prefocusing lens is very dependent on the position and strength of the lens. Some results are shown in *fig. 6*. This gives contours of the normalized spot diameter as a function of the distance from the crossover and the strength of the lens. With the lens very close to the crossover the spot diameter can be reduced to about 55% of the value without prefocusing.

The effect of selective prefocusing can be illustrated by a 'phase-space diagram' for a plane close to the crossover and perpendicular to the tube axis. This is a plot of the angle ϕ between the electron rays and the tube axis against the distance R to the centre, i.e. the intersection of the tube axis with this plane. In the ideal case, where the crossover is a point, all the rays pass through the centre and the phase-space diagram is part of a straight line along the ϕ-axis. In practice, however, most of the rays do not pass through the centre (see fig. 2), so that R varies. The magnitude of this variation depends on the size of the crossover and on the plane of the phase-space diagram. For focusing with the main lens we are interested in the plane for which imaging on the phosphor screen gives the smallest spot; this plane is called the object plane of the main lens. This is not the plane for which the diameter of the crossover is a minimum; because of the spherical aberration in the main lens this plane is further away from this lens.

Fig. 7 shows the phase-space diagram of the object plane with no selective prefocusing and with an optimum selective prefocusing lens. With no selective prefocusing the rays with the highest ϕ-values (the outer rays) pass through the centre exactly ($R = 0$), while the rays with half that ϕ-value have the highest R-value. With selective prefocusing the angle of the outer rays is reduced, while the effect on the rays near the centre is small. The largest angles now correspond to the intermediate rays, which means that the inner and outer rays have been interchanged.

The 'acceptance curves' are also shown, to explain the effect on the spot size a little more clearly. These curves indicate the combinations of R and ϕ that correspond, after focusing by the main lens, to the same radius at the screen, proportional to the R-value at $\phi = 0$. From the acceptance curves that enclose the phase-space diagram it is therefore possible to derive a measure for the spot diameter. From the curves given in fig. 7 it can be seen that selective prefocusing gives a maximum reduction in spot diameter of 46%.

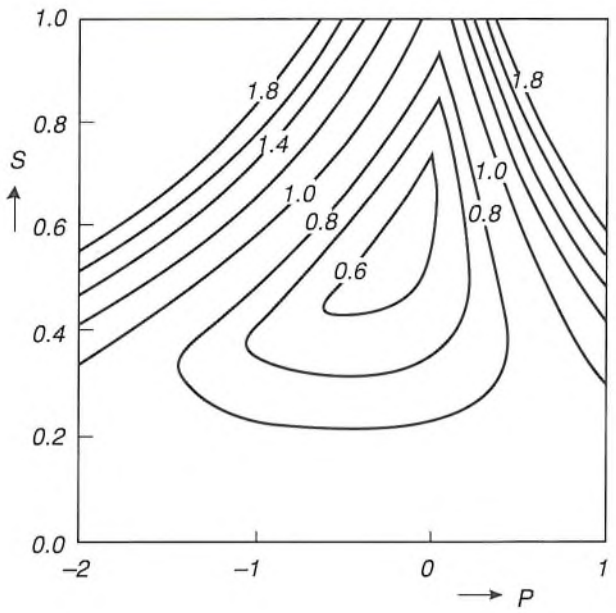

Fig. 6. Calculated contours for the spot diameter, normalized to the value without prefocusing, as a function of the position P of the selective prefocusing lens (with respect to the crossover) and of the strength S of this lens (in arbitrary units). At a position very close to the crossover the spot diameter can be reduced to about 55% of the original value.

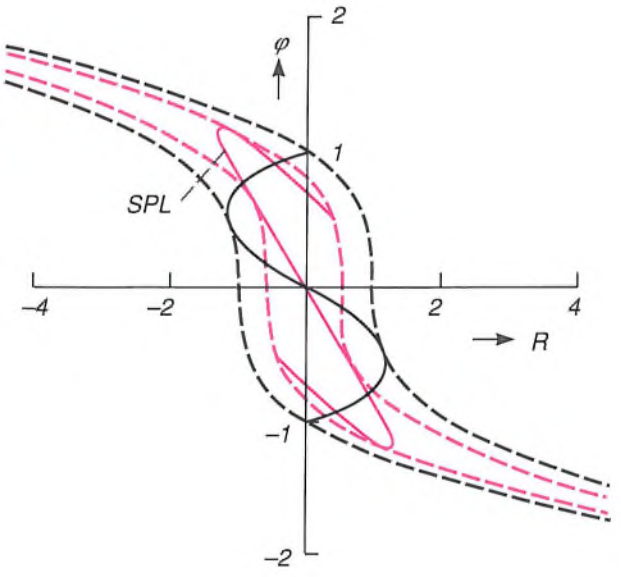

Fig. 7. Calculated phase-space diagrams (continuous lines) for the object plane of the main lens, both with and without an optimum selective prefocusing lens (*SPL*), and the corresponding acceptance curves (dashed lines). In these diagrams the angle ϕ between the rays and the axis of the tube is plotted against the distance R to the centre of the beam. With the selective prefocusing lens the outer rays (the rays with the highest ϕ) make a smaller angle to the axis and the rays at the centre make a larger angle. The acceptance curves indicate the combinations of R and ϕ that correspond to a particular diameter of the spot at the screen; this diameter is proportional to the distance between the curves at $\phi = 0$. By comparing this distance for the two cases it can be shown that the spot diameter is reduced by 46% with the selective prefocusing lens.

When selective prefocusing is used, the contribution from the space-charge effect to the spot size is also reduced. This is due to a change in the intensity distribution in the beam. In conventional guns this distribution resembles the distribution at the cathode: very inhomogeneous, with a high intensity at the centre of the beam and a very low intensity at the edge. With selective prefocusing the weak outer rays are turned inwards, so that the intensity distribution in the beam becomes more uniform. When the intensity distribution is more uniform the space-charge effect makes a smaller contribution to the spot size.

The new electron-optical design

The beam-forming section

In the new electron-optical design the beam-forming section has been made so versatile that the beam diameter and the position and strength of the selective prefocusing lens can easily be modified by changing the potential of one or more of the electrodes. The design makes full use of the expertise gained in dealing with the crossover, the spherical aberration and the space-charge effect described earlier. The design is also based on the 'cup' model for the cathode lens [7], which can be used for calculating the characteristics of the crossover as a function of a single geometrical parameter, the ratio of the distance l between the cathode and the end of the first electrode g_1 to the radius r of the emission region. The geometry and potentials required and the nature of the phase-space diagram at the crossover can be derived from the calculations, which take account of the space-charge effect.

The triode in the new design has an impregnated cathode [3] that gives a maximum current density of $10\,A/cm^2$. This means that an emission region with a radius r of 0.2 mm is large enough to give a maximum beam current of 5 mA. The radius of the cylindrical aperture in the first electrode g_1 is also made 0.2 mm, so that the emission region is no greater than this aperture at the maximum beam current. Since the optimum position of the selective prefocusing lens is very close to the crossover, the second electrode g_2 should not have too high a potential and should be close to g_1. To ensure that sufficient field-strength could nevertheless be obtained at the cathode, we used a very small value, 0.075 mm, for the spacing between g_1 and the cathode and for the thickness of g_1, so that the geometrical parameter l/r for the cup model is 0.75. Using this value in the calculations gives a crossover at 0.56 mm from the cathode. This value sets the maximum distance between the cathode and the end of g_2, since the first electrode of the selective prefocusing lens must be close to the crossover. The thickness of g_2 and its spacing from g_1 have both been set at 0.15 mm.

Two electrodes are used for selective prefocusing. The first electrode (g_3) is located only 0.25 mm from g_2 and has a low potential. The second electrode (g_4) is located more than 1 mm further away and has a much higher potential, which forms a transition to the high potential (about 30 kV) of yet another electrode, which is connected to the screen, the 'screen electrode' (g_5).

The geometry of the beam-forming section in the new design is shown in the diagram of *fig. 8*. Some

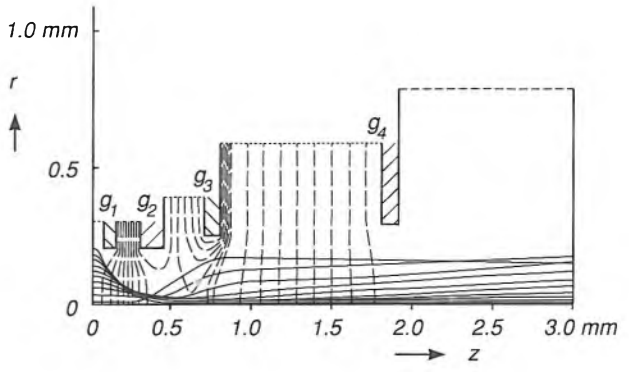

Fig. 8. Geometry of the beam-forming section in the new design of gun, where z is the distance to the cathode and r is the distance to the axis. The electrodes g_1 and g_2, which determine the formation of the crossover, are very thin and are very closely spaced, and are located a short distance away from the cathode. Close to these is another very thin electrode g_3. This electrode and the electrode g_4 form the selective prefocusing lens. Dashed lines: calculated equipotentials when the potentials of g_1, g_2, g_3 and g_4 are -1, 500, 200 and 5000 V respectively. Continuous lines: calculated electron trajectories in this field, with a beam current of about 5 mA. The outer rays of the beam are forced inwards by the selective prefocusing.

equipotential lines are also shown, as well as some calculated trajectories for electrons travelling through the potential field of the electrodes. For clarity the figure only shows electron trajectories that start at right angles to the cathode surface and are unaffected by the space-charge effect. It can be seen from these electron trajectories that selective prefocusing does indeed occur: just beyond the crossover the outer rays are forced towards the inner regions of the beam.

The electron-trajectory data can be more easily analysed by calculating the phase-space diagram for the object plane. The calculated phase-space diagram for six values of the beam current is shown in *fig. 9*. At the highest current the shape of the diagram is very close to the shape required for optimum imaging

[7] A. A. van Gorkum, The cup model for the cathode lens in triode electron guns, Optik 71, 93-104, 1985.

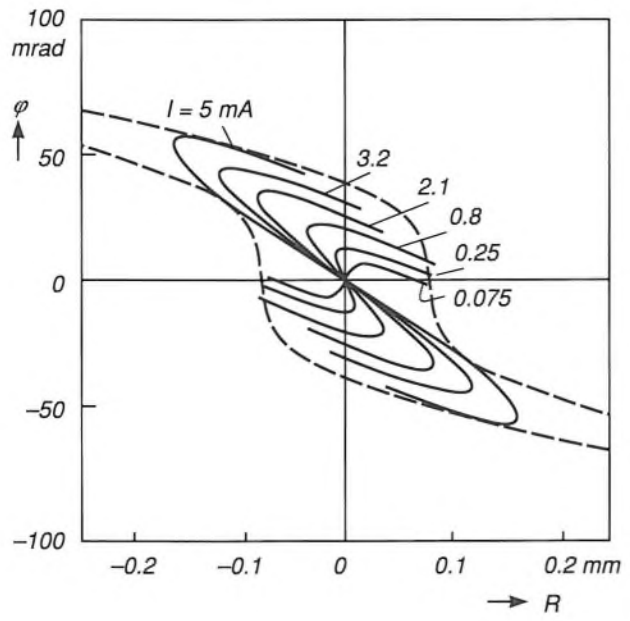

Fig. 9. Calculated phase-space diagrams (continuous lines) for the new design at the object plane of the main lens, for six values of the beam current I, and acceptance curves (dashed lines) for a particular size of spot. The shape of the diagrams depends strongly on I: at lower currents the maximum value of ϕ is much lower than at 5 mA. All the diagrams fit inside the acceptance curves shown except at $I = 0.8$ mA.

(fig. 7). At lower currents this is no longer the case, because of the shift of the crossover with respect to the selective prefocusing lens. At the lowest current some of the rays are in fact focused by this lens: the angle of these rays becomes zero or changes sign. This means that they cross the axis because of the selective prefocusing. Comparison of the phase-space diagrams with the calculated acceptance curves for a particular spot size (see fig. 9) shows whether this affects the imaging. At high currents the phase-space diagram fits inside the acceptance curves, but not when the current is reduced to 0.8 mA. At the two lowest currents the diagram fits inside again. This means that outer rays crossing the axis will not make the spot larger than for the larger currents. A slight increase in spot size as a function of current will occur for currents of about 0.8 mA.

Further calculations have shown that the potential of g_3 has a considerable effect on the shape of the phase-space diagram, especially on the behaviour of the outer rays of the beam. A lower value for this potential gives stronger selective profocusing.

The electrons also pass through the lens formed by g_4 and the screen electrode g_5. In the new design electrons travelling from g_4 to g_5 are exposed to the effect of a weak negative lens. The strength of this lens, and hence the diameter of the beam, can be varied by altering the potential of g_4.

The main lens

For the main lens in the new design we decided to use an electromagnetic lens, of the type shown in fig. 3*a*. Our choice was based on the results mentioned earlier of the calculations of the spherical aberration with various kinds of lens. The calculations showed that for a given size of tube an electromagnetic lens can have a smaller spherical aberration than electrostatic lenses, since its diameter can be larger.

A description of the geometry and operation of the main lens can be found in fig. 1 and fig. 3*a*. The cylindrical yoke for magnetic focusing has an internal diameter of 50 mm and a gap with a width of 10 mm. The centre of the lens is located 95 mm from the cathode and 175 mm from the inside of the phosphor screen.

Construction

An important feature of the design is that the electrodes g_1, g_2 and g_3 are very thin and very closely spaced (see fig. 8). In making the experimental guns special construction techniques were necessary to produce this kind of configuration. We used a method in which the electrodes were soldered to partly metallized sapphire rods. The very small spacings required can be produced and maintained with this method.

The rest of the gun was manufactured by conventional methods, with the electrodes held in position by glass insulator rods. A photograph of the gun is shown in *fig. 10*. The electrodes g_1, g_2 and g_3 cannot be separately distinguished in the photograph. The electrodes g_4 and g_5, the glass rods that support them and the first part of the connection to the screen are clearly visible, however.

The cathode-ray tubes that have been made have a screen diagonal of 125 mm, a deflection angle of 55° and a neck diameter of 36 mm. In most of the experiments the screen was coated with a fine-grain green-

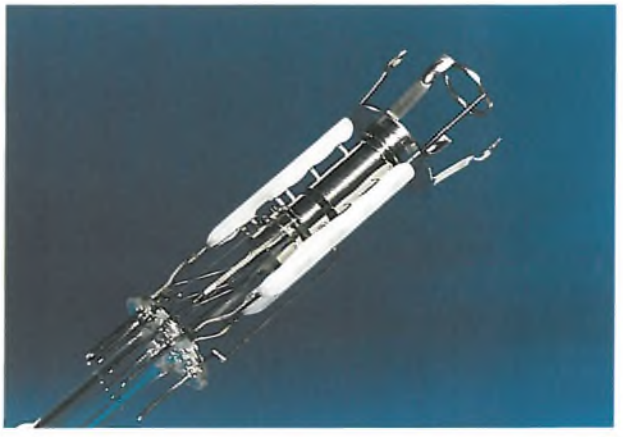

Fig. 10. The new design for the electron gun.

Fig. 11. Cathode-ray tube with the electron gun of fig. 10. The length of the tube is about 300 mm; the neck diameter is 36 mm and the screen diagonal is 125 mm.

emitting phosphor (LaOBr:Tb) applied at high packing density to reduce light scattering in the phosphor layer. A photograph of the tube, also showing the electromagnetic main lens, is shown in *fig. 11*.

Measurements

We have made a large number of measurements on both the guns and the completed tubes to determine the characteristics of interest for projection television. The measurements on the guns were mainly concerned with the phase-space diagrams for the beam. The spot size for the tubes was determined, as well as the picture resolution obtained. The measurements were made with various combinations of electrode potentials and currents. We shall now discuss the most important results briefly.

Phase-space diagrams

Detailed phase-space diagrams for the beam as it emerges from the beam-forming section were measured in a special system [8]. Because of experimental limitations, the same value (7 kV) was used for the potentials of g_4 and g_5, so that there was no lens action between these electrodes. The diagrams were measured for various values of the beam current and the potential of g_3. Some results obtained at the optimum value of the potential of g_3 and three values of the beam current are shown in *fig. 12*. The shape of the diagrams is very dependent on the beam current, as would be expected from the results of the calculations (fig. 9). At 3 mA the diagram has the shape required for optimum selective prefocusing. At 1 mA the outer rays are pulled inwards towards the centre of the beam; some of these rays are almost parallel to the axis of the tube ($\phi = 0$). At the smallest current (0.2 mA) the diagram looks quite different; an intermediate crossover is formed by the selective prefocusing.

The diagrams for the object plane of the main lens can be derived from the measured phase-space diagrams. The object-plane diagrams are in good agreement with the calculated diagrams shown in fig. 9. These results confirm that the introduction of a variable lens close to the crossover does indeed provide the desired selective prefocusing. It can also be seen that this lens is strong enough to modify the phase-space diagrams in the appropriate way.

Resolution

The resolution of the picture is determined by the diameter of the electron spot at the screen. We have measured this at various values of the electrode potentials and beam current, and also as a function of the focusing current, i.e. the current in the coil of the electromagnetic main lens. We have determined the spot diameter as the distance between the points where the intensity is 5% of the maximum value. From the measurements at various values of the potentials of g_3 and g_4 it was possible to derive the combination of potentials that gives the smallest spot diameter.

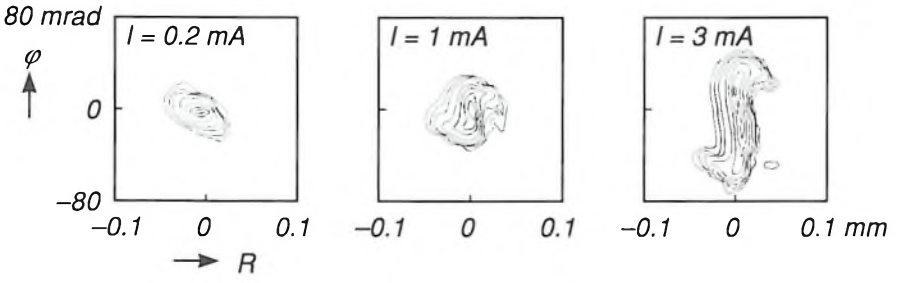

Fig. 12. Measured phase-space diagrams for optimum selective prefocusing, for three values of the beam current I. The contours shown correspond to 2, 5, 10, 25, 50, 75 and 90% of the maximum intensity at the centre. The measured change in shape with beam current corresponds to the results of the calculations.

[8] M. H. L. M. van den Broek, Experimental emittance diagrams of triode electron guns, J. Phys. D 19, 1401-1419, 1986.

Fig. 13 shows the variation as a function of the focusing current for this optimum combination, at various values of the beam current. The focusing current at which the smallest spot is obtained is only slightly dependent on the beam current. This means that there are no undesirable effects if the beam current is fixed, as in normal practice.

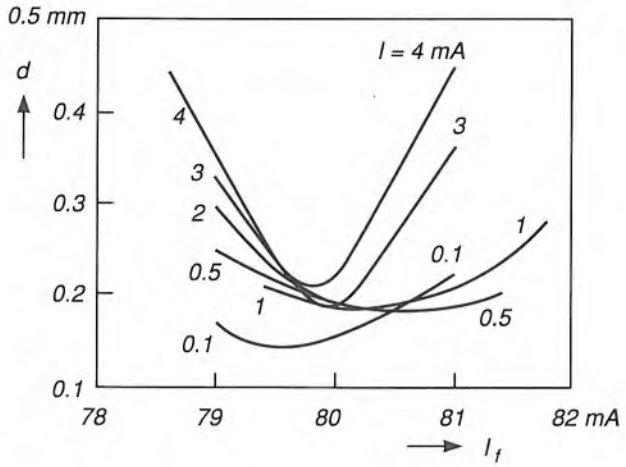

Fig. 13. Measured spot diameter d (distance between the points at 5% of the maximum intensity) as a function of the focusing current I_f, for various values of the beam current I. The beam current does not have much effect on the minimum of the curves.

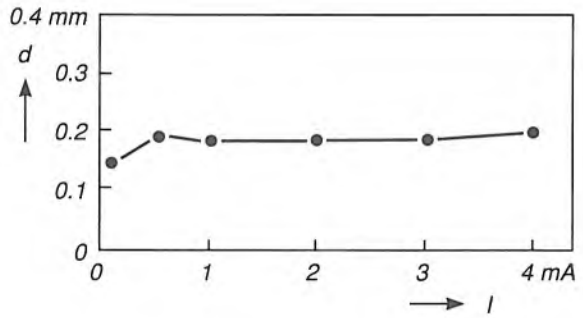

Fig. 14. The spot diameter d measured at a fixed focusing current, as a function of the beam current I. The slightly smaller diameter at the lowest current and the small increase at 0.8 mA are in good agreement with the calculated phase-space diagrams of fig. 9. Even at the highest current the spot diameter is smaller than 0.210 mm.

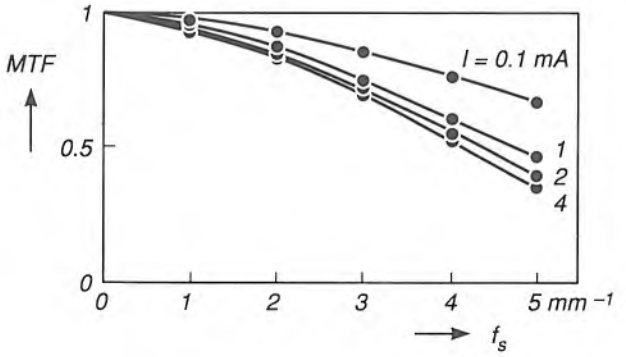

Fig. 15. Modulation transfer function MTF plotted against the spatial frequency f_s (the spatial frequency is the number of periods per mm) at four values of the beam current I. The MTF, a measure of picture resolution, decreases more rapidly with frequency as the beam current increases. At a current of 4 mA and a spatial frequency of 5 mm^{-1} the MTF is still about 40%.

Under optimum conditions with a fixed focusing current the measured spot diameter varies very little with beam current; see *fig. 14*. As would be expected from the phase-space diagrams, the measured spot diameter at low currents is rather smaller and there is a slight enlargement at about 0.8 mA. At currents up to 4 mA the measured spot diameter remains smaller than 0.210 mm. In practice the spot diameter is even less, since the light scattering in the phosphor layer also contributes to the spot size in these measurements. A rough estimate of this contribution indicates that the true spot diameter is no larger than 0.185 mm, and a very sharp image of the crossover is therefore produced.

This has been confirmed by determining the 'modulation transfer function' (or MTF). The MTF represents the fraction of the amplitude transmitted for a sinusoidal signal at a particular spatial frequency. (The spatial frequency is the number of periods per unit length.) *Fig. 15* shows the MTF-value as a function of the spatial frequency for an optimum tube, for four values of the beam current and a fixed focusing current. In assessing these results we have to remember that for a standard PAL television picture on a screen with a 125-mm diagonal a spatial frequency of 2.5 periods per mm corresponds to a signal at 5 MHz. It can be seen that even at a current of 4 mA twice as much horizontal information (5 periods per mm) can be displayed with an MTF of about 40%. This value of the MTF is more than adequate for a good picture.

To sum up, electron guns based on the new design will give cathode-ray tubes with a very high resolution. Tubes that have been made give pictures whose brightness and resolution are sufficient for projection television and high-definition television (HDTV) with large screens.

Important contributions to the work described here were made by M. R. T. Smits and T. L. van Soest. The guns and tubes were made by F. A. M. Habraken and other colleagues in the Tube, Glass and Cathode department. The phosphor coatings in the tubes were applied by colleagues at Philips GmbH Forschungslaboratorium Aachen.

Summary. Electron guns of a new design have been made for application in cathode-ray tubes for projection television. These guns contain an impregnated cathode, a selective prefocusing lens and an electromagnetic main lens. The electron spot on the phosphor screen can be very small, even at high beam currents (0.185 mm at 4 mA), mainly because of selective prefocusing. This means that the brightness and resolution will be sufficient for high-definition projection television.

A diagnostic X-ray tube with spiral-groove bearings

E. A. Muijderman, C. D. Roelandse, A. Vetter and P. Schreiber

The technological development of a product usually advances in a series of small steps. But not always — one example is the change from fixed to rotating anodes in diagnostic X-ray tubes in about 1930. This was a development in which Philips played a leading part, largely because of the work of Albert Bouwers[*]. Since then there has been a steady stream of small improvements in diagnostic X-ray tubes, mostly because problems with limited bearing life and inadequate cooling of the anode have led designers to make modifications. It now looks as though there has been another great leap forward in solving these problems: spiral groove anode bearings lubricated by liquid metal.

Introduction

A diagnostic X-ray tube has to deliver a large amount of radiation from the smallest possible area of the anode, the 'point focus', in a time of several milliseconds to several seconds [1]. The quantity of radiation must be large enough for a sufficient number of electrons to be released at the input screen of an X-ray intensifier tube [2], or to produce sufficient blackening in an X-ray-sensitive film after development. The efficiency of the conversion of electrical energy into X-radiation is less than 1%. More than 99% of the energy supplied to the tube is therefore released in the anode material as heat. In a stationary anode the material would melt locally because the heat is concentrated at the point focus. The problem can be solved by making the anode rotate, since the heat is then spread out over an annular area.

In Philips diagnostic X-ray tubes the surface of the rotating anodes is now made of tungsten alloyed with rhenium. Since the melting point of this alloy is above 3000 °C, high thermal loads at the anode are possible. Alloying with rhenium prevents hairline cracks.

So that the anode can rotate it must be provided with bearings and driven by an electric motor, which has to be an induction motor. The anode, the bearings and the rotor of the induction motor are located inside the evacuated tube. The bearings therefore have to meet a number of rather special requirements. The lubricant for the bearings must not contaminate the vacuum of the tube, the bearings must be able to stand up to high temperatures and they must be electrically and if possible thermally conductive. Solid-metal lubricated ball bearings were therefore always used. The lubricant now used in the high-load Philips diagnostic tubes is silver or lead, applied to the bearing components by special techniques.

Although diagnostic tubes have been produced in this way in large numbers for years, and the technique is still in use, considerable effort is being deployed in the search for alternative methods of providing bear-

Dr Ir E. A. Muijderman was formerly with Philips Research Laboratories, Eindhoven; C. D. Roelandse is with Philips Research Laboratories, Eindhoven; Dipl.-Phys. A. Vetter and Dr P. Schreiber are with Philips Medizin Systeme GmbH, Hamburg.

[*] A. Bouwers, Eine Metallröntgenröhre mit drehbarer Anode, Verh. D. Röntgen-Ges. Vol. 20, suppl. to Fortschr. Röntgenstr. **40**, 102-106, 1929;
J. H. van der Tuuk, X-ray tubes with rotating anode (Rotalix tubes), Philips Tech. Rev. **8**, 31-41, 1946.

[1] W. Hartl, D. Peter and K. Reiber, A metal/ceramic diagnostic X-ray tube, Philips Tech. Rev. **41**, 126-134, 1983/84.

[2] B. van der Eijk and W. Kühl, An X-ray image intensifier with large input format, Philips Tech. Rev. **41**, 137-148, 1983/84.

ings for the anode. The main reason for this is the limited life of the ball bearings, which operate in vacuum under extreme conditions, with forces even higher than those in the bearings in the stabilizer flywheels used in space vehicles [3], which also have to operate in vacuum. Another problem is that the usual methods for calculating the life of ball bearings can only be used if these bearings are grease or oil lubricated. Both are not possible in vacuum.

Because of the limited life of the ball bearings the anode is only rotated during the actual exposure. The anode is therefore run up to the maximum speed very quickly: within one to three seconds. The maximum speed will be about 3000 or 9000 revolutions per minute, depending on the tube type, at a mains frequency of 50 Hz. Once the maximum speed has been reached the actual exposure is made; a high electrical current now flows briefly and heat is developed. The anode is then decelerated very rapidly. The electric motor must be capable of developing a very large driving or decelerating torque, because the anode has a high moment of inertia and has to be accelerated and decelerated very quickly. The 'air gap' between rotor and stator is partly outside the actual tube and is wider than 10 mm because of the high voltage between rotor and stator. This means that the electric motor also has to meet some rather special requirements [1].

Accelerating and decelerating the anode for every exposure means that radiologist and patient are forced to accept delays, which are inconvenient for both and may be uncomfortable for the patient. The time required for accelerating the anode is also a problem if the exposure has to be made at a particular phase of a periodic movement, such as the peristaltic movement of the alimentary tract.

Another disadvantage of ball bearings is that they are noisy, since they contain no grease or oil to attenuate the sound. An even greater disadvantage is that ball bearings present a high thermal resistance to the heat to be conducted away from the anode to the outside world. The heat flow that leaves the tube by conduction through ball bearings is therefore virtually negligible, and amounts to only about 3 W. This means that the rest of the heat flow must leave the anode by radiation, which results in a large increase in the mean anode temperature. The last disadvantage of ball bearings that we shall mention is that they present a varying resistance to the anode current.

Another possibility is to use magnetic bearings [4] for the anode. The advantage here is that no lubricant is necessary, since the shaft is 'floating'. However, the equilibrium of the floating shaft is unstable, so that a comprehensive — and therefore expensive — electronic control circuit is necessary. Since such a circuit can fail (e.g. if the electricity supply fails), which may cause damage, special ball bearings have to be provided that can take over from the magnetic bearings. If these ball bearings are suddenly brought into service they will be subjected to a large acceleration, so that their life is very limited. In practice, this means that the control electronics for the magnetic bearings should never be allowed to fail. Another difficulty with magnetic bearings is that there is no possibility of removing heat by conduction. Also, 'slip rings with carbon brushes' have to be used for the anode-current supply. (It is also possible to use the principle of the thermionic diode for the passage of current from the stationary tube wall to the rotating anode shaft.) Because of these problems — and also because of the complicated construction of the magnetic bearing — no diagnostic X-ray tubes with magnetic bearings have yet appeared on the market.

Fig. 1. The new Philips MRC200 diagnostic X-ray tube with an anode mounted in spiral-groove bearings lubricated by liquid metal. The anode diameter is 200 mm. The rated input is 85 kW[7].

At Philips Research Laboratories in Eindhoven another solution has been found to the problem of providing bearings for the rotating anode of a diagnostic X-ray tube: spiral-groove bearings with liquid metal as the lubricant. The application of these bearings solves all of the problems mentioned above:

- life,
- noise,
- heat transfer and
- current supply.

The heat conduction of a metal-lubricated spiral-groove bearing is about a thousand times greater than

that of a ball bearing. Another extremely important advantage is that an anode with spiral-groove bearings can rotate continuously, since its life is virtually unlimited. Periodic acceleration and deceleration are then no longer necessary. This means that radiologist and patient will no longer be subject to delays and that the motor can be much simpler, since it only has to supply enough power to keep the anode rotating continuously. Moreover, a spiral-groove bearing can support a much greater load than a ball bearing, so that an anode of much greater diameter can be used. Since the anode only has to be run up to speed once each day, in the morning, the higher moment of inertia is not a problem.

A spiral-groove bearing is a self-acting bearing, i.e. a bearing that requires no external pressure source, in which there are grooves in one of the two bearing surfaces [5]. If the relative movement of the bearing surfaces is in the correct direction, the grooves ensure that the lubricant is retained in the bearing. Since the space between the two cylindrical surfaces is wedge-shaped and because of the propulsive action of the grooves an excess pressure is produced in the lubricant. If the excess pressure is high enough, the lubricant will keep the bearing surfaces apart. The principle of the spiral-groove bearing has been known for twenty or thirty years and various forms of these bearings have been studied in depth [6] at Philips Research Laboratories.

For the application of a spiral-groove bearing in a diagnostic X-ray tube it was necessary to find an alloy that is liquid at or near room temperature and can be used as a lubricant. The alloy must also have a low vapour pressure at high temperatures, so that the vacuum in the tube is not contaminated by vaporized metal. Mercury is therefore unsuitable as a lubricant in vacuum. After extensive experiments by J. Gerkema and J. B. Pelzer at Philips Research Laboratories a gallium alloy was eventually found that can act as a lubricant.

The study at Philips Research Laboratories laid the foundations for a diagnostic X-ray tube that has recently been introduced by Philips Medizin Systeme GmbH of Hamburg. The new tube is shown in *fig. 1*. The type designation MRC 200 is related to the external diameter of the anode, 200 mm. In the present version the anode rotates at almost 3000 rev/min. The rated input power of the tube is 85 kW [7]. The metal-lubricated spiral-groove bearings have been put through extensive life tests at Philips Research Laboratories. A preproduction batch of tubes has been produced at Hamburg, and these have been thoroughly tested.

The new tube was specially designed for making cine exposures. These are of interest in the investiga-

a

b

c

Fig. 2. Earlier generations of Philips diagnostic X-ray tubes. *a*) The SRO 90 tube, *b*) the SRM 100 tube and *c*) the SRC 120 tube. The numbers refer to the anode diameter in mm.

[3] J. P. Reinhoudt, A flywheel for stabilizing space vehicles, Philips Tech. Rev. **30**, 2-6, 1969;
J. Crucq, The reaction wheels of the Netherlands satellite ANS, Philips Tech. Rev. **34**, 106-111, 1974.

[4] E. M. H. Kamerbeek, Magnetic bearings, Philips Tech. Rev. **41**, 348-361, 1983/84.

[5] Strictly speaking the journal bearings are *helical*-groove bearings, but the term 'spiral-groove bearing' is in fact widely used for both spiral-groove thrust bearings and helical-groove journal bearings.

[6] E. A. Muijderman, New forms of bearing: the gas and the spiral groove bearing, Philips Tech. Rev. **25**, 253-274, 1963/64;
E. A. Muijderman, G. Remmers and L. P. M. Tielemans, Grease-lubricated spiral-groove bearings, Philips Tech. Rev. **39**, 184-198, 1980.

[7] The rated input power is defined as the power that can be supplied for a maximum of 0.1 second to a tube that was in thermal equilibrium at a continuous power input of 250 W.

tion of bloodvessels where the blood flow is very rapid, as in the coronary arteries (coronary angiography). At a relatively low radiation dose for each exposure, 6 to 10 series of exposures, each consisting of 300 to 600 exposures, are made for each patient at a rate of 25 to 100 exposures per second. Until recently it was necessary to wait for a fairly long time between the series of exposures until the heat stored in the anode had been dissipated by radiation. The great advantage of an anode with a large diameter combined with metal-lubricated spiral-groove bearings is not only that a large amount of heat can be stored in the anode, but also that this heat can be removed by conduction. The radiologist is therefore no longer forced to wait for the anode to cool down during an investigation. This means that the patient does not have to be subjected to the investigation procedures for such a long time. This can be a great advantage, especially where catheters are used, since more power is then required from the tube. Nor is it necessary to use so much contrast agent. An important economic advantage, of course, is that more patients can be dealt with in a given time.

Besides the version for cine exposures, other versions of the new tube will also be developed for other applications where the excellent cooling and the continuously rotating anode will be advantages. Another advantageous feature of the new tube is the spatial stability of the focus. Because the temperature remains low, the position of the focus never changes by more than 50 μm. The stability of the focus is of interest for the digital processing of X-ray images. With the 'subtraction' method, for example, bloodvessels can be made visible by 'taking away' an image made without a contrast agent from one made with a contrast agent.

Fig. 2 shows the earlier types of tube with rotating anodes: the SRO 90, with glass envelope, the SRM 100, with an envelope of glass and metal, and the SRC 120, made entirely from metal and ceramics [1]. The numbers in these designations indicate the diameter of the anode in mm; the speed of rotation is almost 9000 rev/min for all the tubes. The introduction of each new tube meant a step in the improvement of the performance. It can be seen from *fig. 3* that the introduction of the newest tube corresponded to a much larger advance than the previous ones. The bar chart shows the relative value of various quantities, with the SRM 100 glass/metal tube as the basis for comparison. These quantities are the rated input power [7], the maximum load during a single cine pulse, the product of heat capacity and mean anode temperature, the quantity of heat that can be stored in the anode during a comparable series of cine exposures (lasting 6 to 10 seconds), the total heat loss due to radiation and conduction, and the total energy that can be supplied to the tube during a cine investigation lasting 20 minutes. The bar chart shows that this last figure is more than three times higher than for earlier tube types.

We shall now look at the construction of the tube. Next we shall consider the anode bearings, and finally we shall briefly touch on certain aspects of the dynamic stability of the rotating anode.

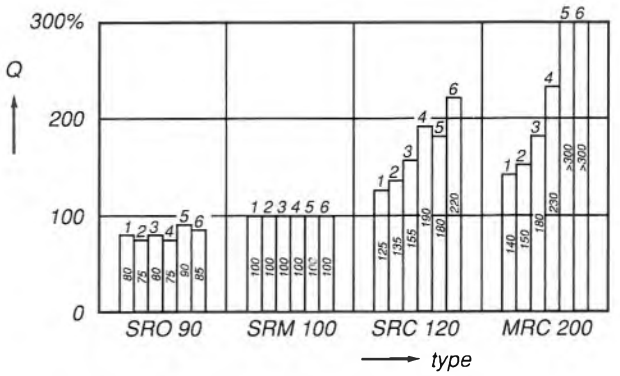

Fig. 3. Bar chart giving a comparison of the performance of successive generations of diagnostic X-ray tubes, see also figs 1 and 2. The relative values Q of a number of quantities are plotted for four different tubes, with Q for the SRM 100 tube given a value of 100 in each case. The values quoted for each type of tube are: *1* the rated input power [7], *2* the maximum load during a single cine pulse, *3* the product of heat capacity and mean anode temperature, *4* the quantity of heat that can be stored in the anode during a comparable series of cine exposures (lasting 6 to 10 seconds), *5* the total thermal energy that can be dissipated by radiation and conduction, and *6* the total energy that can be supplied to the tube during a cine investigation lasting 20 minutes.

The construction of the tube

Fig. 4 shows a cross-section of the new MRC 200 diagnostic X-ray tube in its shield. The space between tube and shield is filled with oil, which provides high-voltage insulation. The oil also takes part in the cooling process by taking up the heat leaving the anode (A) by radiation and conduction through the spiral-groove bearing (SGB); oil pumped through the tube O_1 is directed against the bottom of the opening in the bearing.

The electrons emitted by the filament of the cathode (K) strike the anode at the point focus (PF). The X-radiation produced here is confined to a conical beam (X) by diaphragms (not shown). The X-radiation leaves the tube through an extremely thin beryllium window (W), a thin layer of oil and a thin aluminium window (Al) in the shield.

The difference between the temperature at the point focus and the mean anode temperature is approx-

imately inversely proportional to $\sqrt{nD}$, where n is the speed of rotation and D is the outer diameter of the anode [1]. In designing an X-ray tube with a rotating anode it is necessary to find the right compromise between speed of rotation and anode diameter. In this tube, mainly intended for cine exposures, it was decided to make the speed fairly low and the anode diameter large. In earlier tubes a large anode diameter was undesirable, since running up to speed and decelerating would have taken too long because of the high moment of inertia. In the new tube this is no problem, since it only happens once in each working day. The anode of the MRC 200 therefore has both a high moment of inertia and a high heat capacity. This means that a large amount of heat can be stored temporarily in the neighbourhood of the circular path of the point focus. This heat can then be dissipated quickly by conduction through the bearing.

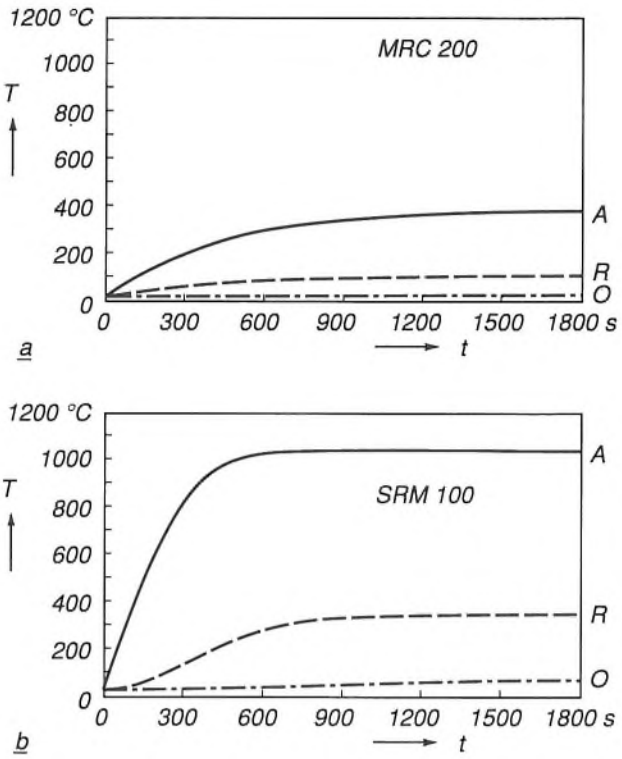

Fig. 5. The temperature T as a function of time t for continuous operation at an input power of 1 kW, starting at time $t = 0$, for *a*) the new MRC 200 tube and *b*) the earlier type, the SRM 100. *A* the temperature variation at the anode circumference, *R* at the rotor circumference and *O* of the oil in the shield.

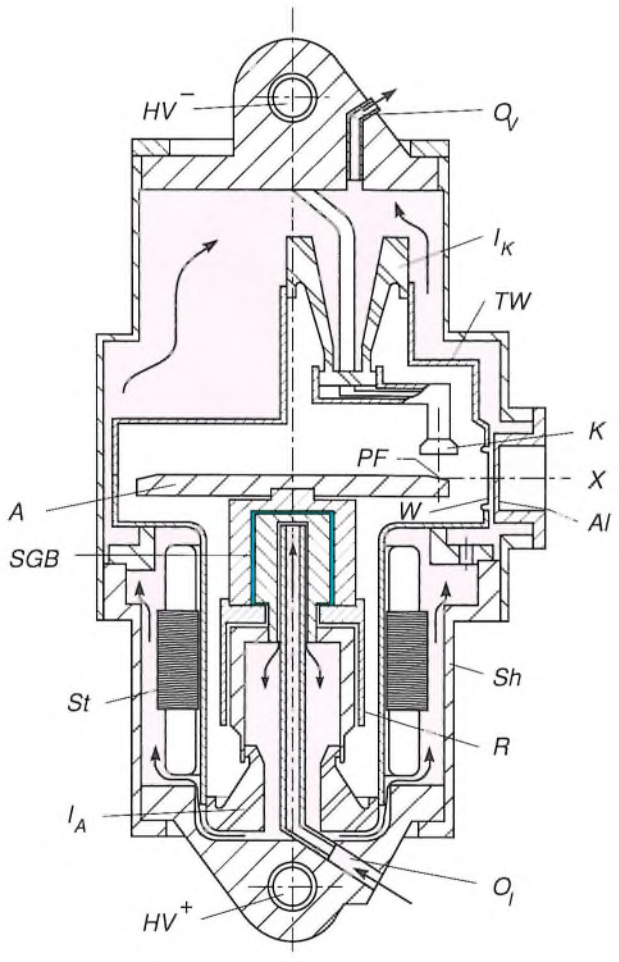

Fig. 4. Schematic cross-section of the MRC 200 diagnostic X-ray tube. White: vacuum. Red: oil; the direction of flow is indicated by arrows. HV^+ positive high-voltage connector. I_A ceramic insulator for the anode. *St* stator of the induction motor that rotates the anode. *SGB* spiral-groove bearing to take up forces in both radial and axial directions. (The liquid metal is shown as a blue line.) *A* anode. HV^- negative high-voltage connector. O_V oil outlet. I_K ceramic insulator for the cathode. *TW* metal envelope. *W* beryllium window. *K* cathode. *X* X-ray beam (the diaphragms that confine the beam are not shown). *Al* aluminium window. *Sh* shield. *R* rotor of the induction motor. O_I oil supply. *PF* point focus.

It can be seen from *fig. 5* that the heat capacity of the anode and the heat dissipation by conduction are significantly better than for the earlier SRM 100 tube. The figure shows the results of a computer simulation of the temperature variation in the anode after starting at a continuous tube loading of 1 kW with a relatively large focus. The three curves relate to the temperatures of the anode rim, the rotor and the oil in the shield. All the temperatures for the MRC 200 are considerably lower than for the SRM 100. Since the temperature increase at the anode rim is so much smaller in comparable circumstances, the energy load at the focus can be much higher.

The new tube, like its predecessor, is made entirely of metal and ceramics, and contains no glass at all. Ceramic components can be more accurately dimensioned. The metal envelope is at earth potential. This avoids difficulties from the charge effects that occur in tubes that contain glass in the envelope. The highest potential difference across either of the ceramic insulators (I_K at the cathode and I_A at the anode, see

fig. 4) is about 75 kV, half the maximum voltage across the tube. The high-voltage connectors, HV^+ and HV^-, are located at the two ends of the shield. The connectors are connected to the spiral-groove bearing and the filament of the cathode respectively, and are insulated from the shield by plastic insulators.

As noted earlier, the rotor (*R*) of the induction motor and the spiral-groove bearing are located in the vacuum. The stator (*St*) is located outside the tube in the oil between the tube and the shield. Since the anode rotates continuously, the maximum motor power does not have to be much higher than is necessary to overcome the friction in the spiral-groove bearings. The friction loss is only about 40 W.

The anode bearings

The anode spiral-groove bearing, *SGB* in fig. 4, is constructed as a bearing with a stationary shaft and a rotating bearing bush. Since it has to be possible to use the X-ray tube in all possible orientations, the spiral-groove bearing system consists of two thrust bearings and two journal bearings [5]; see *fig. 6*. The pumping action of the different components cancels out, so that no lubricant is forced out of the bearing. This is achieved by using herringbone groove patterns, which give the greatest build-up of pressure at the centre of each pattern. Since there are groove patterns for thrust-bearing action on both upper and lower sides, axial forces can be taken up in two directions. The two separate journal bearings with their own helical groove patterns are necessary for taking up torques as well as forces.

Fig. 6 also shows a diagram of the 'pressure hills' of the different parts of the bearing: the pressure in the lubricant as a function of position. This figure holds for the bearing system in a centric position. When the bearing positions itself eccentrically because of the radial load, the height of the pressure hills is also a function of the angle in the circumferential direction. The peak of the pressure hill is found just in front of the position where the bearing gap is smallest. Integrating each pressure hill gives a part of the bearing force. In principle it makes no difference to the operation of a spiral-groove thrust bearing whether the grooves are in the stationary part of the bearing or in the moving part. In fact we put the grooves in the moving part of the bearing to facilitate production.

Dynamic stability of the rotating anode

An investigation has also been made at Philips Research Laboratories into the possibility of instability of the rotating anode because of a whirling motion of the axis of symmetry. This 'half-omega whirl' has an angular frequency about half that of the rotational speed. Although this instability can be investigated by using a computer program [8], results obtained in this way do little to improve the physical understanding of the problem. This means that the search for the correct settings for the various parameters that can affect the stability of a new design — there are 32 of them — has to be made virtually 'in the dark'.

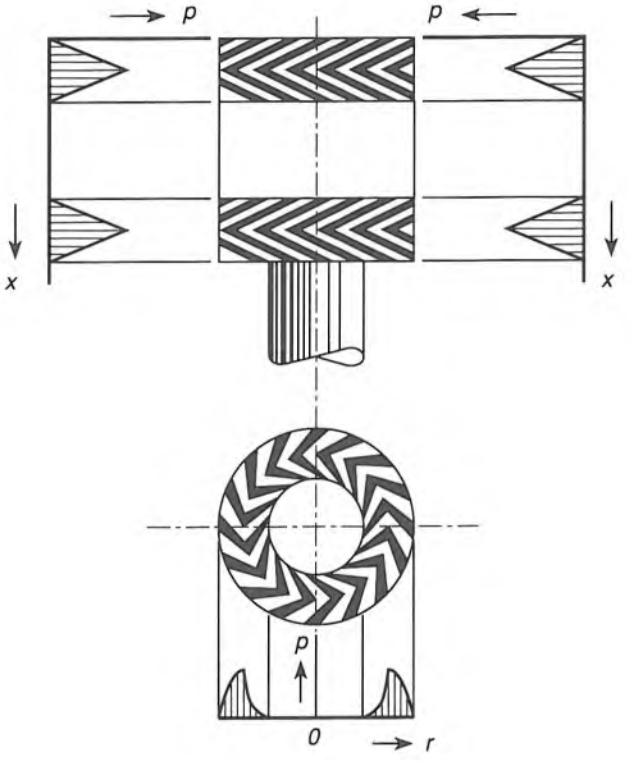

Fig. 6. The spiral-groove bearing system. *Above:* the helical groove patterns of the journal bearings. *Below:* the spiral groove pattern in one of the thrust bearings. The same groove pattern is used in the other thrust bearing (mirror symmetry). The hatched areas are 'pressure hills', representing the pressure p in the lubricant, as a function of x for the journal bearings in a centric position, and as a function of r for the thrust bearing.

In earlier investigations [8] a simple stability condition in the form of an analytical expression was derived for a rotor whose bearings are attached to the environment by rigid supports. Since the connection between the spiral-groove bearing via the envelope to the environment is not rigid, we cannot use this simple stability condition.

Fortunately, however, the rotating X-ray-tube anode has a number of symmetries that greatly simplify the problem of stability with flexible bearing supports. It was therefore possible to find an analytical expression for this case as well: a simple relation

for the 'critical speed', the speed at which any increase in speed would lead to the whirling action mentioned above [9]. The differences between computer calculations and the results of using this simple relation are generally no more than a few per cent. It also turns out that the familiar assumption that the critical speed is twice the lowest resonant frequency of the rotor is by no means true in all cases.

We have used the analytical stability condition that we have derived to test the stability of the anode of the MRC 200 tube. The positive results obtained are in complete agreement with practical tests. It will also be possible to use the method for rapid and early prediction of the likelihood of rotor instabilities in future designs. The physical understanding that results from the relation derived earlier will then indicate methods of avoiding instabilities.

Summary. Spiral-groove bearings can replace the ball bearings in the vacuum of a rotating-anode diagnostic X-ray tube. This increases the maximum load the tube can take and solves a number of other problems, such as limited bearing life, difficulties with anode cooling and noise from the bearings. The spiral-groove bearing has to be lubricated with liquid metal, partly because the vapour pressure of the lubricant should be low, partly because it must conduct the anode current. A gallium alloy has been found to be a successful lubricant. In the new Philips MRC 200 diagnostic X-ray tube with spiral-groove bearings more than three times as much energy can be handled during a complete cine investigation as in the SRM 100 tube of the previous generation. This means that an investigation of this type takes only half as long with the new tube, so that there are economic advantages as well as reduced patient stress.

[8] J. P. Reinhoudt, On the stability of rotor-and-bearing systems and on the calculation of sliding bearings, Thesis, Eindhoven 1972.

[9] E. A. Muijderman, Algebraic formulas for the threshold and mode of instability and the first critical speed of a simple flexibly supported (overhung) rotor-bearing system, Proc. Conf. on Rotordynamics, Tokyo 1986, 201-210.

Scientific publications

These publications are contributed by staff from the laboratories and other establishments that form part of or are associated with the Philips group of companies. Many of the articles originate from the research laboratories named below. The publications are listed alphabetically by journal title.

Philips GmbH Forschungslaboratorium Aachen, Weißhausstraße, 5100 Aachen, Germany — *A*

Philips Research Laboratory, Brussels, 2 avenue Van Becelaere, 1170 Brussels, Belgium — *B*

Philips Natuurkundig Laboratorium, Postbus 80000, 5600 JA Eindhoven, The Netherlands — *E*

Philips GmbH Forschungslaboratorium Hamburg, Vogt-Kölln-Straße 30, 2000 Hamburg 54, Germany — *H*

Laboratoires d'Electronique Philips, 3 avenue Descartes, 94450 Limeil-Brévannes, France — *L*

Philips Laboratories, N.A.P.C., 345 Scarborough Road, Briarcliff Manor, N.Y. 10510, U.S.A. — *N*

Philips Research Laboratories, Cross Oak Lane, Redhill, Surrey RH1 5HA, England — *R*

Philips Research Laboratories Sunnyvale P.O. Box 9052, Sunnyvale, CA 94086, U.S.A. — *S*

A. H. van Ommen, J. J. M. Ottenheim, A. M. L. Theunissen & A. G. Mouwen *E*	Synthesis of heteroepitaxial $Si/CoSi_2/Si$ structures by Co implantation into Si	Appl. Phys. Lett. **53**	669-671	1988
A. P. M. Kentgens, A. H. Carim & B. Dam *E*	Transmission electron microscopy of thin $YBa_2Cu_3O_{7-x}$ films on (001) $SrTiO_3$ prepared by dc triode sputtering	J. Cryst. Growth **91**	355-362	1988
A. H. Boonstra & T. N. M. Bernards *E*	The dependence of the gelation time on the hydrolysis time in a two-step SiO_2 sol-gel process	J. Non-Cryst. Solids **105**	207-213	1988
A. J. E. M. Janssen *E*	On exponentially weighted Toeplitz matrices and their use in the analysis of a frequency-domain, power-compensated adaptive filter	Linear circuits, systems and signal processing: theory and application, C.I. Byrnes *et al.* (eds), Elsevier Science, Amsterdam	207-216	1988
B. J. van Wees*, L. P. Kouwenhoven*, H. van Houten, C. W. J. Beenakker, J. E. Mooij* (**Univ. of Technol., Delft*), C. T. Foxon & J. J. Harris *E,R*	Quantized conductance of magnetoelectric subbands in ballistic point contacts	Phys. Rev. B **38**	3625-3627	1988
J. C. M. Henning & J. P. M. Ansems *E*	Photoionization threshold of the deep donor in Si-doped $Al_xGa_{1-x}As$	*ibid.*	5772-5775	1988
L. W. Molenkamp, G. E. W. Bauer, R. Eppenga & C. T. Foxon *E,R*	Exciton binding energy in (Al,Ga)As quantum wells: effects of crystal orientation and envelope-function symmetry	*ibid.*	6147-6150	1988
A. H. Carim, A. F. de Jong & D. M. de Leeuw *E*	Ordering phenomena in the tetragonal superconductor $CaBaLaCu_3O_{7-\delta}$	*ibid.*	7009-7012	1988
A. K. Niessen, A. R. Miedema, F. R. de Boer (*Univ. Amsterdam*) & R. Boom (*Res. Labs, Hoogovens-Groep, IJmuiden*) *E*	Enthalpies of formation of liquid and solid binary alloys based on 3d metals. IV. Alloys of cobalt	Physica B **151**	401-432	1988
G. Keesman *E*	Motion estimation based on a motion model incorporating translation, rotation and zoom	Signal processing IV: theories and applications, J.L. Lacoume *et al.* (eds), Elsevier Science, Amsterdam	31-34	1988
R. N. J. Veldhuis *E*	Adaptive restoration of unknown pixels in digital images	Signal processing IV: theories and applications, J.L. Lacoume *et al.* (eds), Elsevier Science, Amsterdam	1469-1472	1988

Subject index, Volumes 36-44

Figures in bold type indicate the volume number, figures in ordinary type indicate the page number. Subjects dealt with in volumes **1-35** are listed in the indexes included with volumes **10, 15, 20, 25, 30, 35** and **40**. The asterisk * indicates that the entry refers to a photograph and caption.

Author index, Volumes 36-44

Figures in bold type indicate the volume number, and those in ordinary type the page number. Articles published in volumes **1-35** are given in the author indexes at the end of volumes **10, 15, 20, 25, 30, 35** and **40.**

B. A. G. van Luyt and L. E. Zegers, The Compact Disc Interactive system,
PhilipsTech.Rev.**44**,No.11/12,326-333,Nov.1989.

The standard for the CD-I system (Compact Disc Interactive) for consumer applications is an extension of the standard for CD-ROM (Read-Only Memory) for professional applications for computers, which in turn is an extension of the standard for CD-DA (Digital Audio). The CD disc contains images, sound, text, and the associated software in digital form. The information is organized in sectors on the disc, each with its own address and a list of contents. There are two levels of error correction, four quality levels for sound and three quality levels for images. This means that quality can be traded against storage capacity and bit rate when the disc is created. The supplier of interactive programs does this by means of an authoring system. The output from the authoring system is the digital information used in manufacturing the 'mother disc'.

T. G. Spanjer, A. A. van Gorkum and W. M. van Alphen, Electron guns for projection television,
PhilipsTech.Rev.**44**,No.11/12,348-356,Nov.1989.

Electron guns of a new design have been made for application in cathode-ray tubes for projection television. These guns contain an impregnated cathode, a selective prefocusing lens and an electromagnetic main lens. The electron spot on the phosphor screen can be very small, even at high beam currents (0.185 mm at 4 mA), mainly because of selective prefocusing. This means that the brightness and resolution will be sufficient for high-definition projection television.

R. Raue, A. T. Vink and T. Welker, Phosphor screens in cathode-ray tubes for projection television,
PhilipsTech.Rev.**44**,No.11/12,335-347,Nov.1989.

Phosphor screens in tubes for projection television have to meet some critical requirements, since they operate at much higher electron-excitation densities than the screens in conventional direct-view tubes. Their light output should be only slightly sublinear at high excitation densities and should be stable under prolonged intense electron bombardment. This affects the selection of the phosphors and the screen processing. The preparation of screens with the optimum light output and resolution requires a careful evaluation of their optical properties and degradation behaviour.

E. A. Muijderman, C. D. Roelandse, A. Vetter and P. Schreiber, A diagnostic X-ray tube with spiral-groove bearings,
PhilipsTech.Rev.**44**,No.11/12,357-363,Nov.1989.

Spiral-groove bearings can replace the ball bearings in the vacuum of a rotating-anode diagnostic X-ray tube. This increases the maximum load the tube can take and solves a number of other problems, such as limited bearing life, difficulties with anode cooling and noise from the bearings. The spiral-groove bearing has to be lubricated with liquid metal, partly because the vapour pressure of the lubricant should be low, partly because it must conduct the anode current. A gallium alloy has been found to be a successful lubricant. In the new Philips MRC 200 diagnostic X-ray tube with spiral-groove bearings more than three times as much energy can be handled during a complete cine investigation as in the SRM 100 tube of the previous generation. This means that an investigation of this type takes only half as long with the new tube, so that there are economic advantages as well as reduced patient stress.

OTHER PHILIPS PUBLICATIONS

Philips Journal of Research

An English-language journal with articles on research at the various Philips Laboratories. Six issues per volume.
Information: Philips Journal of Research, Philips Research Laboratories, P.O. Box 80 000, 5600 JA Eindhoven.

Acta Electronica

An annual publication with a special subject for each year, with articles in French and English on electronics and applied physics.
Information: Acta Electronica, Laboratoires d'Electronique et de Physique appliquée, 3 Avenue Descartes, 94451 Limeil-Brévannes Cedex, France.

Philips Telecommunication and Data Systems Review

An English-language journal, dealing with developments, systems, and products in business communications, computers, computer networks, telecommunications services, radio communications and dictation equipment. Four issues per volume.
Information: Philips Telecommunication and Data Systems Review,
P.O. Box 32, 1200 JD Hilversum, The Netherlands.

Electronic Components and Applications

An English-language journal with articles dealing with electronic components and materials and their applications. Four issues per volume.
Information: Electronic Components and Applications, Philips Electronic Components and Materials Division, P.O. Box 218, 5600 MD Eindhoven, The Netherlands.

Medicamundi

An English-language journal with articles on radiology, isotope diagnosis and medical electronics. Three issues per volume.
Information: Medicamundi, Philips Nederland, Boschdijk 525, 5621 JG Eindhoven, The Netherlands.

Philips Tech. Rev. Vol. 44, No. 11/12, Nov. 1989

Contents

PHILIPS TECHNICAL REVIEW
Philips Research Laboratories
P.O. Box 80000
5600 JA Eindhoven
The Netherlands

Printed in the Netherlands